Theses and Dissertations   1. Thesis and Dissertation Collection, all items

1947

Lateral stability of thin tapered struts

Durup, Paul Christian; Weisenberg, Joseph O.

Pasadena, California; California Institute of Technology

http://hdl.handle.net/10945/6485

GUGGENHEIM AERONAUTICAL LABORATORY

CALIFORNIA INSTITUTE OF TECHNOLOGY

LATERAL STABILITY

OF THIN TAPERED STRUTS

Thesis by

Lieut. Paul C. Durup, USN

Lieut. Joseph O. Weisenberg, USN

-1947-

FORM AL-5 12M 9-41

LATERAL STABILITY

OF THIN TAPERED STRUTS

Thesis by

Lieut. Paul C. Durup, USN

and

Lieut. Joseph O. Weisenberg, USN

Thesis
D9

ACKNOWLEDGEMENT

TABLE OF CONTENTS

I. SUMMARY

From the experimental investigation detailed herein it has been determined, at least for two types of struts, that there is a very close correlation between (1) the experimentally determined buckling load which a given strut will sustain and (2) the critical load determined by the use of Southwell's method, which does not entail loading the strut to its critical load. By using an initial eccentricity and loads considerably less than the critical, the critical load may be derived from the results of three or four simple test readings, not requiring an elaborate or refined setup.

Experimental verification of existing theory of lateral buckling is noted for the case of struts tapered to a point at the application of the loading.

The possibility of determining the eccentricity of a given loading by plots of β/p vs β is pointed out and the type of curve to be expected is noted. However due to lack of refinement of the experimental setup, no definite conclusions are presented.

The theoretical portion of this thesis offers the derivation of a formula for the lateral buckling of a thin linearly tapered strut of constant thickness. Due to the complexity of the problem certain simplifications were made to facilitate this derivation.

Comparison of the values determined by use of this formula with the values experimentally determined for four struts shows a fairly close correlation.

It is suggested that in some future work a more thorough investigation be made of the relation between the eccentricity of the loading and the load which a strut will carry, using a given deflection as a parameter.

II. INTRODUCTION

In aeronautical design there are several instances in which the lateral stability of thin tapered struts is of importance. Specifically one might mention as examples: (1) exposed wind tunnel struts, and (2) airplane external antenna masts. In each case it is extremely important that the thinnest possible section be used in order to reduce disturbance of the air flow and hence drag, to a minimum. At the same time it is required to carry as high a load as possible without buckling or deflecting excessively.

Very little literature or experimental data on this particular problem of lateral stability has been published and most theoretical treatises deal only with the general problem and do not consider specific applications. This lack of information is even greater for eccentrically loaded or truncated struts.

As a thesis project it was proposed to make some experimental tests on struts of various planforms and thickness ratios. In addition it was proposed to develop formulas which might be used in calculating critical buckling loads for lateral stability of (1) thin struts tapered to a theoretical point at the point of application of loading and (2) thin struts, tapered but truncated.

The purpose of the experimental work was largely three-fold.

(1) Timoshenko, Reference 1, referring to a German report by Federhofer, Reference 2, gives formulae which give the critical buckling load of a thin strut where the depth of cross section varies according to the law:

Reference 1: S. Timoshenko, "Theory of Elastic Stability", p. 249-250 McGraw-Hill, 1936.

Reference 2: K. Federhofer, "Reports International Congress of Applied Mechanics", Stockholm, 1930.

-5-

$$h = h_o \left(1 - \frac{z}{\ell} \right)^n$$

whore

h = depth at root

ℓ = length

z = coordinate along length

n = some value which corresponds to type of taper.

The critical buckling load is given as:

$$P_{cr} = \frac{m \sqrt{B_1 \, C}}{\ell^2}$$

whore

B_1 and C = flexural and torsional rigidities of fixed end

of a cantilever strut

m =   factor depending upon 'n' above and upon type

of loading.

It was desired to check these results experimentally and this was done

for two aluminum models of thickness/depth ratios of 1/48 and 1/36 at

the root.

(2) It was desired to obtain experimental buckling loads of trun-

cated thin struts which could be checked with critical loads to be worked

out theoretically. Aluminum and steel models of thickness/depth ratio

1/28 at root and 1/4 at the tip were tested experimentally.

(3) Southwell, Reference 3, has indicated a method of determining

the critical load from test data within the elastic regime. All models

have been subjected to this analysis.

Reference 3: R. V. Southwell, "Proceedings Royal Society", London,
series A, Vol. 135, p. 60, 1932.

In addition the Southwell lines determined as above will intersect the axis of deflections at a certain value α_i which is a function of the eccentricity of the loading in our case. α has been plotted against eccentricity in an attempt to establish a relationship between the two.

The method of procedure and results obtained are noted in sections III and IV below.

Theoretical results are noted in section V.

III. EXPERIMENTAL APPARATUS

A. TEST SPECIMENS

All test specimens were of the same type being cut from
1/8" (approximately) sheet cold rolled steel or 24 ST aluminum.
All struts were designed for an effective length (from edge of end
support to point of loading) of 18", with varying degrees of taper
from varying root depths. Thickness remained essentially constant
throughout, though it would perhaps have been desirable to have
models with taper in two directions.

At no point in the models was shear found to be critical.
However in designing the ends of the models to carry the knife edge
it was necessary to carry the knife edge support back along the model
far enough to obtain sufficient depth to resist the bending moment
in the yz plane.

See Appendix A for drawings of all models:

Model A   4.5" root depth, aluminum, tapered to point

Model B   6.0" root depth, aluminum, tapered to point

Model C   3.5" root depth, aluminum, truncated

Model D   3.5" root depth, steel, truncated

B. DESCRIPTION OF PHYSICAL SETUP

See Appendix B and C for drawings and photographs of setup.

A first consideration was to obtain complete end fixity as
nearly as possible. The models were heavily bolted by means of two
steel 2 x 2 x 1/4 angles, one on each side, to a heavy permanent steel
backplate. The flange faces on opposite sides of the model were scored
heavily so that when the through bolts were tightened the flanges would
bite into the models. It is believed complete end fixity was obtained,
for throughout the tests the indicators returned to zero when the load

was removed, except as hereinafter noted.

Care was taken to mount the model with the y-axis vertical and the z-axis horizontal.

A second consideration was to obtain the desired loading at the desired point. By mounting the z-axis of symmetry horizontal and by applying the load in a vertical direction, a loading perpendicular to the strut axis was assured. The strut and knife edge were designed so that the loading edge would be on the axis of symmetry. In addition it was desired to have a transverse x-axis motion of the knife edge to provide for eccentricity of loading. Use of set screws as shown in the knife edge detail allowed this eccentricity to be introduced. (Note: In this experiment the eccentricity adjustment was not very precise, since the set screws imbedded themselves into the models to a varying and unmeasureable degree. In addition, there was a tendency of the screws to climb on the model when turning and of thus twisting the knife edge. A suggested alternate screw design is shown for future work. Also it is suggested that some means for keeping the knife edge aligned with the z-axis be introduced). To allow the knife edge to seat more easily on the model, the surface of the model was grooved, giving, in effect, two parallel lines of contact for the knife edge to seat on.

The loading was accomplished simply by hanging weights in a pan, through a saddle, over the knife edge. To avoid dynamic loading and to prevent buckling failure prematurely, a jack was provided under the weight pan to apply or relieve loading.

A fourth consideration was to measure deflections. Angular deflections, due to their greater ease of measurement, were chosen rather than downward or sidewise deflections, as the deflection

parameter in all considerations. It was felt that a simple mechanical pointer would suffice if sufficient magnification were provided. Consequently a 30" arm was clamped securely on the edge of each specimen, the arm being demountable so that the same pointer could be used on successive models. A piece of millimeter graph paper was mounted behind each end of the pointer with its coordinates in the vertical and horizontal directions. In order to obtain a measure of the angle of twist of the model it was only necessary to measure the difference in the vertical deflection between the two ends of the pointer. This effectively considers the angle as being directly proportional to the sine of the angle. This approximation is valid for the small angles which we are measuring. The millimeter graph paper was adjusted for each model so that the pointers would read zero in each coordinate before application of load. It was found that the position of the pointer could be estimated to 1/10th of a millimeter. Side deflections of the model caused one end of the pointer to rub on the indicating panel, thus introducing a slight stabilizing moment. This moment was considered negligible due to the use of a pointer of very small rigidity.

C. TESTING PROCEDURE

The model was set up in the rig as indicated in B above, and the reading scales set so that the pointers read zero. Loading was applied in varying increments depending upon the size of the model and upon the proximity of the applied to the critical loads. This first loading was to determine the experimental critical load for strut, or the maximum centrally applied load which strut would support with deflection in the yz-plane only, and above which the slightest external disturbance would cause the strut to buckle. The knife edge was first placed at the approximate center of the model. As loads were applied

the model would tend to deflect sideways in one direction, or the other. Accordingly the knife edge would be moved by means of the adjustment set screws, in a direction opposite to the motion. This adjustment was made with the load largely relieved by means of the jack. Then the load was applied again and the process repeated until downward deflection only was noted. Additional weights were added until another side deflection was noted, and the knife edge adjustment process repeated. Finally a load was reached where the slightest movement of the knife edge in either direction would cause the strut to buckle in that direction. This load was taken as the experimental critical load, and the position of the knife edge as the zero position, for that strut setup.

The knife edge was always shifted with some, but not all, load applied to facilitate seating of the knife edge on the strut. Before loads were applied or taken off, the jack underneath the pan was used to take the load from the knife edge and hence from the strut. Following the locating of the zero point of the knife edge for the particular model setup, a certain amount of eccentricity of loading was introduced by shifting the knife edge. As weights were added, readings were taken, at various loading stages, of the accumulated loading and of the position of the pointers in the y and x directions on the indicating paper. Then the eccentricity was increased and the procedure repeated. This process was carried out until the knife edge was located almost at the edge of the model.

Since it was not desired to exceed the yield strength in these models the angle of twist had to be held within some limits, except in the final runs. The readings were roughly plotted as they were made and when the flat of the curves of difference versus load was reached,

no further reading were taken.

Between each change of eccentricity, zero readings on the pointer were checked to be certain of complete end fixity and the absence of yielding.

IV. EXPERIMENTAL RESULTS

A. DATA

1. Tabular Form

Pages 15 to 45 present data in tabular form. The different runs represent different eccentricities as noted, and the data is presented in six columns as follows:

(1) Cumulative loading = P.

(2) Reading in the y-direction of the left end of the pointer in millimeters.

(3) Reading in the y-direction of the right end of the pointer in millimeters.

(4) Reading of either right or left end of the pointer in the x-direction in millimeters.

(5) Difference between readings of the two ends of the pointer in millimeters. NOTE: This difference (DIFF.) as has been pointed out, is taken as directly and linearly related to the angle of twist β, and is used in place of β. The units of DIFF. are millimeters. A plot of DIFF. vs β is included in appendix D.

(6) Difference divided by the cumulative loading = DIFF./P. This column has not been calculated for all runs.

Page 45 contains tabular data of eccentricity and c_i (see Introduction) for the various models. This data is taken from charts B, D, F and H, and from the tabular data.

2. Graphical Form

Figures A to I (pages 46 to 54) show results in graphical form. All of the tabular data has not been plotted since many curves would be largely coincident. Illustrative curves are shown.

Again, DIFF. stands for difference which is directly proportional to the angle of twist β (see Appendix D), and the units of DIFF. are millimeters.

Curves are labeled as RUN 1, etc. These terms correspond to various eccentricities which vary for the different runs for different models. However eccentricity increases as the run numbers increase.

Figure E shows curves running to what might be considered a negative difference. This was due to a reversal noted on this model. At low eccentricities and loads the model began to twist in one direction and then switched its direction of twist as the load was increased. This was considered due to initial twist in the model.

Figure I shows graphical form of eccentricity vs c_i.

Model A

Aluminum   4.5" root depth   -0-" tip depth   0.125" thickness

(1)	(2)	(3)	(4)	(5)	(6)
Critical Run Eccentricity = = 0"					
8.5					
33.6					
44.0					
54.3					
64.5					
69.5					
70.0					
70.5					
71.0					

(1)	(2)	(3)	(4)	(5)	(6)
Run 1 Eccentricity = . = 0.00195					
33.6	-0.2	-2.3	-0-	2.1	.0625
44.0	-0.2	-2.9	-0-	2.7	.0614
49.0	-0.2	-3.4	-0-	3.2	.0653
54.3	-0.1	-3.9	-0-	3.8	.0700
59.3	0	-4.4	+0.1	4.4	.0742
61.3	+0.2	-4.8	0.2	5.0	.0815
63.3	0.4	-5.2	0.4	5.6	.0884
65.5	1.1	-6.0	0.6	7.1	.1084
66.5	1.6	-6.4	1.0	8.0	.1203

(1)	(2)	(3)	(4)	(5)	(6)
Run 1 (cont'd) Eccentricity =				= 0.00195"	
67.5	2.3	-7.3	1.5	9.6	.1423
68.5	3.7	-8.7	2.4	12.4	.1810
69.0	4.8	-9.9	3.2	14.9	.2130
69.5	7.2	-12.2	4.5	19.4	.2790

(1)	(2)	(3)	(4)	(5)	(6)
Run 2 Eccentricity =				= 0.00390"	
33.6	0.2	-2.9	-0-	3.1	.0922
44.0	0.7	-3.9	+0.2	4.6	.1046
54.3	1.2	-5.2	0.4	6.4	.1180
59.3	1.9	-6.3	0.8	8.2	.1384
61.3	2.4	-6.9	1.3	9.3	.1513
63.3	3.2	-7.9	1.5	11.1	.1752
64.5	3.9	-8.8	2.1	12.7	.1969
65.3	4.7	-9.6	2.6	14.3	.2180
66.0	5.2	-10.0	3.0	15.2	.2300
66.5	5.9	-10.8	3.3	16.7	.2510
67.0	6.7	-11.6	3.7	18.3	.2732
67.5	7.7	-12.6	4.5	20.3	.3005

(1)	(2)	(3)	(4)	(5)	(6)
Run 3	Eccentricity =			= 0.00586"	

(1)	(2)	(3)	(4)	(5)	(6)
33.6	0.8	-3.2	-0-	4.0	.1191
44.0	1.2	-4.3	-0.2	5.5	.1251
54.3	2.2	-6.2	-0.6	8.4	.1548
59.3	3.2	-7.7	-1.3	10.9	.1838
61.3	3.9	-8.4	-1.7	12.3	.2006
63.3	4.9	-9.8	-2.5	14.7	.2320
64.5	6.1	-10.8	-3.2	16.9	.2620
65.5	7.2	-12.0	-3.8	19.2	.2932
66.0	7.9	-12.8	-4.3	20.7	.3154
66.5	8.9	-13.9	-4.9	22.8	.3428

(1)	(2)	(3)	(4)	(5)	(6)
Run 4	Eccentricity =			= 0.00780	

(1)	(2)	(3)	(4)	(5)	(6)
33.6	1.2	-3.7	-0.2	4.9	.1458
44.0	1.8	-5.0	-0.4	6.8	.1546
49.0	2.2	-5.9	-0.5	8.1	.1652
54.3	3.1	-7.1	-1.0	10.2	.1880
57.3	3.8	-8.1	-1.4	11.9	.2075
59.3	4.5	-8.9	-1.8	13.4	.2260
61.3	5.4	-10.0	-2.4	15.4	.2511
62.3	6.1	-10.7	-2.8	16.8	.2698
63.3	6.9	-11.6	-3.3	18.5	.2920
64.5	8.2	-12.9	-4.0	21.1	.3273
65.0	8.9	-13.7	-4.4	22.6	.3478
65.5	9.8	-14.6	-5.0	24.4	.3722

(1)	(2)	(3)	(4)	(5)	(6)
Run 5	Eccentricity =			= 0.00977"	
38.6	1.3	-3.9	0.2	5.2	.1348
44.0	2.1	-5.3	0.4	7.4	.1681
49.0	2.7	-6.3	0.6	9.0	.1836
54.3	3.7	-7.7	1.2	11.4	.2100
57.3	4.6	-8.8	1.6	13.4	.2337
59.3	5.8	-9.7	2.1	14.9	.2511
61.3	6.3	-10.8	2.6	17.1	.2787
63.3	7.9	-12.6	3.7	20.5	.3237
64.5	9.5	-14.2	4.5	23.7	.3676
65.0	10.2	-14.9	5.1	25.1	.3860

/

(1)	(2)	(3)	(4)	(5)	(6)
Run 6	Eccentricity =			= 0.01170"	
38.6	1.6	-4.0	0.2	5.6	.1667
44.0	2.2	-5.4	0.5	7.6	.1728
49.0	2.8	-6.4	0.7	9.2	.1878
52.0	3.3	-7.2	1.0	10.5	.2019
54.3	3.4	-7.8	1.4	11.9	.2155
56.3	4.3	-8.6	1.5	12.9	.2290
58.3	5.1	-9.3	2.0	14.4	.2470
60.3	6.0	-10.4	2.4	16.4	.2719
62.3	7.4	-11.9	3.2	19.3	.3098
63.3	8.3	-12.9	3.7	21.2	.3348
64.5	9.9	-14.7	4.8	24.6	.3815

(1)	(2)	(3)	(4)	(5)	(6)
	Run 7	Eccentricity =		= 0.01362"	
33.6	1.3	-3.9	0.2	5.2	.1549
44.0	2.1	-5.4	0.4	7.5	.1704
49.0	2.7	-6.2	0.5	8.9	.1818
54.3	3.6	-7.7	1.1	11.3	.2080
59.3	5.1	-9.4	2.1	14.5	.2443
61.3	6.2	-10.8	2.6	17.0	.2772
63.3	7.9	-12.4	3.6	20.3	.3205

(1)	(2)	(3)	(4)	(5)	(6)
	Run 8	Eccentricity =		= 0.02342"	
33.6	1.7	-4.0	0.2	5.7	.1696
44.0	2.3	-5.7	0.4	8.0	.1819
49.0	3.0	-6.7	0.6	9.7	.1981
52.0	3.4	-7.2	1.0	10.6	.2089
54.3	4.0	-8.0	1.4	12.0	.2210
56.3	4.6	-8.8	1.5	13.4	.2380
58.3	5.3	-9.6	2.0	14.9	.2555
60.3	6.3	-10.7	2.6	17.0	.2817
62.3	7.8	-12.2	3.3	20.0	.3212
64.5	10.3	-15.1	5.1	25.4	.3940

(1)	(2)	(3)	(4)	(5)	(6)
Run 9 Eccentricity =				= 0.03125"	
37.6	2.2	−4.6	0.3	6.8	.2023
44.0	3.2	−6.3	0.6	9.5	.2160
40.0	3.9	−7.5	1.0	11.4	.2324
54.3	5.2	−9.1	1.7	14.3	.2654
56.3	5.9	−9.9	2.0	15.8	.2805
58.3	6.9	−11.1	2.6	18.0	.3064
59.3	7.4	−11.8	3.0	19.2	.3289
60.3	8.2	−12.3	3.4	20.5	.3400
61.3	8.9	−13.3	3.8	22.2	.3620
61.8	9.3	−13.8	4.0	23.1	.3740
62.3	9.8	−14.3	4.4	24.1	.3866

(1)	(2)	(3)	(4)	(5)	(6)
Run 10 Eccentricity =				= 0.03905"	
33.6	3.3	−5.8	0.3	9.1	.2708
44.0	4.9	−8.1	1.0	13.0	.2955
47.0	5.8	−9.1	1.3	14.9	.3170
49.0	6.2	−9.8	1.6	16.0	.3262
51.0	6.9	−10.6	2.0	17.5	.3430
53.0	7.7	−11.4	2.3	19.1	.3605
54.3	8.2	−12.1	2.5	20.3	.3735
55.3	8.8	−12.8	2.8	21.6	.3905
56.3	9.3	−13.3	3.2	22.6	.4010
57.3	9.8	−14.0	3.4	23.8	.4150
58.3	10.7	−14.8	3.7	25.5	.4370
59.3	11.3	−15.8	4.2	27.1	.4565

(1)	(2)	(3)	(4)	(5)	(6)
Run 10 (cont'd)		Eccentricity =		= 0.08905	
60.3	12.3	-16.8	4.7	29.1	.4825
61.3	13.4	-18.0	5.4	31.4	.5120
62.3	15.0	-19.7	6.4	34.7	.5570
63.3	17.2	-21.9	7.6	39.1	.6175
64.5	21.3	-26.2	10.0	47.5	.7370
65.0	24.2	-29.2	11.5	53.4	.8210
65.5	buckles				

Aluminum 6" root depth -0-" tip depth 0.125" thickness

(1)	(2)	(3)	(4)	(5)	(6)
	Critical Run Eccentricity =			= 0"	
33.6					
58.8					
69.2					
79.4					
89.2					
91.2					
92.2					
93.2					
94.2					
95.2					
96.2					
97.2					

(1)	(2)	(3)	(4)	(5)	(6)
	Run 1 Eccentricity =			= 0.00195"	
33.6	-0.7	-0.7	-0-	0	.0000
58.8	-0.8	-1.4	0.2	0.6	.0102
69.2	-0.6	-2.0	0.5	1.4	.0202
79.4	+0.3	-3.1	1.4	3.4	.0429
89.2	3.8	-7.1	4.0	10.9	.1344
91.2	6.1	-9.8	5.4	15.9	.1744
92.2	8.5	-12.0	6.9	20.3	.2205
92.7	9.4	-13.5	7.5	22.9	.2470

(1)	(2)	(3)	(4)	(5)	(6)
Run 1 (cont'd)	Eccentricity =			= 0.00195"	
93.2	11.8	-15.5	8.9	27.3	.2935
93.7	13.8	-18.0	10.2	31.8	.3405

(1)	(2)	(3)	(4)	(5)	(6)
Run 2	Eccentricity =			= 0.00390"	
33.6	-0.5	-0.9	-0-	0.4	.0119
58.8	-0.4	-1.7	0.5	1.3	.0221
69.2	+0.2	-2.5	0.7	2.5	.0361
79.4	1.1	-3.9	1.6	5.0	.0630
84.4	2.4	-5.3	2.5	7.7	.0912
86.4	3.3	-6.3	3.3	9.6	.1111
89.2	5.3	-8.7	4.5	14.0	.1569
90.2	6.5	-10.0	5.5	16.5	.1830
91.2	7.8	-11.7	6.3	19.5	.2135
92.2	10.0	-14.2	8.0	24.2	.2625
93.2	13.0	-18.0	10.0	31.0	.3325

(1)	(2)	(3)	(4)	(5)	(6)
Run 3	Eccentricity =			= 0.00586"	
33.6	-0.3	-1.0	0.1	0.7	
58.8	-0.1	-2.0	0.5	1.9	
69.2	+0.3	-2.8	1.0	3.1	
79.4	1.7	-4.2	2.0	5.9	
84.4	3.1	-6.0	2.8	9.1	

(1)	(2)	(3)	(4)	(5)	(6)
Run 5 (cont'd) Eccentricity =				= 0.00586"	
86.4	4.0	-7.1	3.5	11.1	
87.4	4.8	-7.9	4.0	12.7	
88.4	5.4	-8.9	4.5	14.3	
89.2	6.2	-9.9	5.2	16.1	
91.2	9.1	-13.2	7.2	22.3	
92.2	11.4	-16.1	8.6	27.5	
92.7	13.3	-17.9	9.8	31.2	

(1)	(2)	(3)	(4)	(5)	(6)
Run 4 Eccentricity =				= 0.00780"	
35.6	-0.3	-1.1	0.2	0.8	.0258
58.6	+0.1	-2.2	0.5	2.3	.0392
69.2	0.6	-3.1	1.0	3.7	.0534
74.2	1.0	-3.7	1.3	4.7	.0634
79.4	1.9	-4.7	2.0	6.6	.0831
81.4	2.5	-5.2	2.5	7.7	.0946
84.4	3.4	-6.6	3.0	10.0	.1185
86.4	4.4	-7.7	3.5	12.1	.1400
30.4	5.8	-9.3	4.3	15.1	.1710
90.2	7.9	-11.8	6.2	19.7	.2184
92.2	13.1	-16.3	8.8	29.4	.3187
93.2	16.6	-20.2	10.5	36.8	.3945

(1)	(2)	(3)	(4)	(5)	(6)
	Run 5	Eccentricity =		= 0.01170$''$	
33.6	-0.2	-1.1	0.2	0.0	.0268
58.8	+0.2	-2.2	0.5	2.4	.0408
69.2	0.7	-3.1	1.0	3.3	.0549
74.2	1.2	-3.8	1.3	5.0	.0674
79.4	2.1	-4.8	2.0	6.9	.0869
81.4	2.6	-5.4	2.4	8.0	.0983
84.4	3.8	-6.8	3.2	10.6	.1256
86.4	4.9	-8.0	4.0	12.9	.1493
88.4	5.6	-9.8	5.0	15.4	.1743
90.2	9.2	-12.2	6.4	21.4	.2610
91.2	11.2	-14.3	8.0	25.5	.2790
92.2	14.1	-17.6	9.6	31.7	.3440

(1)	(2)	(3)	(4)	(5)	(6)
	Run 6	Eccentricity =		- 0.01362$''$	
33.6	-0.2	-1.2	0.2	1.0	.0295
58.8	+0.2	-2.2	0.5	2.4	.0408
69.2	0.8	-3.2	1.0	4.0	0.578
79.4	2.2	-5.0	2.1	7.2	.0907
84.4	4.1	-6.9	3.3	11.0	.1303
86.4	5.2	-9.1	4.0	14.3	.1656
88.4	6.9	-9.9	5.0	16.8	.1900
90.2	9.4	-12.8	6.7	22.2	.2462
92.2	14.2	-17.7	9.5	31.9	.3460
92.7	15.9	-19.6	10.2	35.5	.3830

(1)	(2)	(3)	(4)	(5)	(6)
	Run 7	Eccentricity =		− 0.01950"	
33.6	−0.1	−1.2	0.2	1.1	
56.8	+0.3	−2.5	0.5	2.8	
69.2	0.9	−3.3	1.0	4.2	
79.4	2.5	−5.2	2.2	7.7	
84.4	4.3	−7.2	3.3	11.5	
86.4	5.4	−3.6	4.0	14.0	
88.4	7.3	−10.4	5.4	17.7	
90.2	9.3	−15.0	6.9	22.8	
92.2	14.6	−18.1	9.6	32.7	
92.7	16.3	−20.0	10.8	36.3	

(1)	(2)	(3)	(4)	(5)	(6)
	Run 8	Eccentricity =		= 0.02342"	
33.6	0.2	−1.2	0.2	1.4	.0417
58.8	1.1	−2.9	0.6	4.0	.0680
69.2	1.9	−4.0	1.3	5.9	.0852
74.2	2.7	−4.9	1.7	7.6	.1025
79.4	3.9	−6.3	2.5	10.2	.1286
81.4	4.7	−7.2	3.1	11.9	.1462
84.4	6.2	−9.8	4.0	16.0	.1395
86.4	7.7	−10.6	5.0	18.3	.2120
88.4	10.0	−12.9	6.5	22.9	.2590
90.2	13.4	−16.7	8.5	30.1	.3350
91.2	16.2	−19.8	10.0	36.0	.3950

(1)	(2)	(3)	(4)	(5)	(6)
	Run 9	Eccentricity =		= $0.02730''$	
33.6	0.3	-1.7	0.2	2.0	
58.8	1.3	-3.4	0.6	4.7	
69.2	2.6	-4.9	1.5	7.5	
74.2	3.4	-5.9	2.0	9.3	
79.4	4.0	-7.3	3.0	12.2	
81.4	5.3	-8.7	3.4	14.5	
84.4	7.5	-10.4	4.5	17.9	
86.4	9.3	-12.4	5.5	21.7	
88.4	11.9	-15.1	7.3	27.0	
89.2	13.2	-16.5	8.0	29.7	
90.2	15.3	-18.3	9.2	34.1	

(1)	(2)	(3)	(4)	(5)	(6)
	Run 10	Eccentricity =		= $0.03125''$	
33.6	1.1	-2.0	0.2	3.1	.0922
58.8	2.7	-4.4	0.8	7.1	.1208
69.2	4.2	-6.3	1.8	10.5	.1517
74.2	5.3	-7.7	2.5	13.0	.1751
79.4	7.3	-9.9	3.7	17.2	.2165
81.4	8.6	-11.1	4.5	19.7	.2420
83.4	9.8	-12.7	5.4	22.5	.2700
85.4	11.8	-14.8	6.5	26.6	.3117
87.4	14.4	-17.8	8.2	32.2	.3685
88.4	16.4	-19.7	9.0	36.1	.4085

(1)	(2)	(3)	(4)	(5)	(6)
Run 11	Eccentricity =			= 0.03515"	
33.6	1.4	-2.6	0.3	4.0	
58.8	3.6	-5.3	1.2	8.9	
69.2	5.3	-7.4	2.2	12.7	
74.2	6.8	-9.1	3.0	15.9	
79.4	9.2	-11.6	4.3	20.8	
81.4	10.3	-13.0	5.2	23.3	
83.4	12.1	-14.8	6.1	26.9	
85.4	13.2	-17.1	7.4	30.3	
87.4	17.3	-20.3	9.1	37.6	

(1)	(2)	(3)	(4)	(5)	(6)
Run 12	Eccentricity =			= 0.03905"	
33.6	1.7	-2.6	0.3	4.3	.1280
58.8	3.8	-5.7	1.3	9.5	.1617
69.2	5.8	-7.9	2.4	13.7	.1979
74.2	7.2	-9.7	3.1	16.9	.2277
79.4	9.8	-12.2	4.5	22.0	.2772
81.4	11.2	-13.8	5.3	25.0	.3072
83.4	12.9	-15.7	6.5	28.6	.3431
85.4	15.2	-18.1	7.8	33.3	.3900
86.4	16.6	-19.8	8.5	36.4	.4210

(1)	(2)	(3)	(4)	(5)	(6)
Run 13 Eccentricity = = 0.04690"					
33.6	1.8	-2.7	0.3	4.5	
58.8	3.9	-5.7	1.2	9.6	
69.2	5.8	-7.9	2.3	13.7	
74.2	7.3	-8.6	3.1	15.9	
79.4	9.8	-12.2	4.5	22.0	
81.4	11.2	-13.7	5.5	24.9	
83.4	12.9	-15.5	6.5	28.4	
85.4	15.2	-18.0	7.5	33.2	

(1)	(2)	(3)	(4)	(5)	(6)
Run 14 Eccentricity = = 0.05466"					
33.6	1.9	-3.0	0.3	4.9	.1459
53.8	4.3	-5.2	1.4	9.5	.1617
69.2	6.5	-8.8	2.5	15.3	.2210
74.2	8.3	-10.5	3.4	18.8	.2530
79.4	11.1	-13.6	5.0	24.7	.3110
81.4	12.6	-15.2	5.8	27.8	.3410
83.4	14.6	-17.2	7.0	31.8	.3810
85.4	16.9	-19.9	8.4	36.8	.4310
87.4	20.3	-23.7	10.2	44.0	.5040
89.2	26.1	-29.5	13.3	55.6	.6230
89.7	29.0	-33.0	15.2	62.0	.6910
90.2	35.2	-39.8	18.5	75.0	.8310
90.7	buckles				

Aluminum   3.5" root depth   0.5" tip depth   .0.127" thickness

(1)	(2)	(3)	(4)	(5)	(6)
Critical Run		Eccentricity =		= 0".	
29.12					
39.32					
49.67					
59.93					
60.93					
61.93					
62.93					
63.93					
64.93					
65.93					
66.93					

(1)	(2)	(3)	(4)	(5)	(6)
Run 1		Eccentricity =		= 0.0015"	
29.12	−1.2	−0.3	0.1	−0.4	.0137
39.32	−1.7	−1.0	0.2	−0.7	.0178
49.67	−2.0	−1.2	0.2	−0.8	.0161
59.93	−2.1	−1.9	0.4	−0.2	.0033
64.93	−1.1	−3.3	1.6	+2.2	.0339
65.93	+0.5	−5.1	3.2	5.6	.0050
66.43	3.1	−7.7	5.2	10.3	.1625

(1)	(2)	(3)	(4)	(5)	(6)
Run 2 Eccentricity = − 0.0026″					
39.12	−1.0	−0.8	0.1	−0.8	.0040
39.52	−1.0	−1.1	0.1	−0.5	.0127
49.67	−1.8	−1.8	0.2	−0.2	.0040
54.67	−1.3	−1.8	0.5	−0.1	.0013
59.38	−1.8	−2.8	0.8	+0.5	.0068
61.98	−1.2	−2.8	1.2	1.0	.0080
62.98	−1.0	−3.1	1.5	2.1	.0884
63.98	−0.4	−3.8	2.0	3.4	.0581
64.98	+0.4	−4.9	2.8	5.8	.0010
65.48	1.5	−5.9	3.5	7.4	.0118
65.98	3.1	−7.7	5.0	10.8	.0164

(1)	(2)	(3)	(4)	(5)	(6)
Run 5 Eccentricity = − 0.0052″					
39.12	−1.0	−1.0	0.1	−0−	
38.52	−1.8	−1.5	0.2	0.1	
49.67	−1.5	−1.9	0.5	0.4	
54.67	−1.4	−2.2	0.8	0.8	
59.38	−0.9	−3.0	1.3	2.1	
61.98	−0.8	−3.6	1.6	3.5	
62.98	+0.1	−4.3	2.2	4.4	
63.98	1.1	−5.2	3.1	6.3	
64.98	2.8	−7.1	4.4	9.0	
65.48	4.2	−8.9	5.6	13.1	

(1)	(2)	(3)	(4)	(5)	(6)
Run 4	Eccentricity =			= 0.0078"	
20.12	-0.9	-1.1	0.1	0.2	.0069
39.32	-1.1	-1.3	0.2	0.2	.0051
49.67	-1.5	-1.9	0.3	0.4	.0080
54.67	-1.3	-2.2	0.6	0.9	.0165
59.93	-0.8	-3.2	1.5	2.4	.0400
61.93	-0.2	-3.9	2.0	3.7	.0596
62.93	+0.3	-4.6	2.3	4.9	.0779
63.93	1.2	-5.6	3.2	6.8	.1063
64.93	3.1	-7.6	4.5	10.7	.1648

(1)	(2)	(3)	(4)	(5)	(6)
Run 5	Eccentricity =			= 0.0104"	
29.12	-0.9	-1.1	0.1	0.2	
39.32	-1.1	-1.4	0.2	0.3	
49.67	-1.3	-1.9	0.3	0.6	
54.67	-1.2	-2.4	0.6	1.2	
59.93	-0.5	-3.3	1.3	2.3	
61.93	+0.1	-4.1	2.1	4.2	
63.93	1.7	-6.0	3.3	7.7	
64.93	3.8	-8.1	5.0	11.9	
65.43	5.4	-10.0	6.5	15.4	

(1)	(2)	(3)	(4)	(5)	(6)
Run 6	Eccentricity =			= 0.0156"	
29.12	-0.9	-1.1	0.1	0.2	.0069
39.32	-1.1	-1.4	0.1	0.3	.0076
49.67	-1.3	-1.9	0.4	0.6	.0121
54.67	-1.1	-2.6	0.6	1.5	.0274
59.93	-0.7	-3.5	1.3	2.8	.0467
61.93	+0.2	-4.2	2.1	4.4	.0711
63.93	1.9	-6.2	3.6	8.1	.1268
64.93	4.0	-8.3	5.3	12.3	.1894
65.43	5.9	-10.7	7.0	16.6	.2538

(1)	(2)	(3)	(4)	(5)	(6)
Run 7	Eccentricity =			= 0.0208"	
29.12	-0.8	-1.1	0.1	0.3	
39.32	-1.0	-1.6	0.2	0.6	
49.67	-1.1	-2.2	0.5	1.1	
54.67	-0.9	-2.7	0.9	1.8	
57.67	-0.8	-3.2	1.2	2.4	
59.93	-0.2	-3.9	1.7	3.7	
60.93	+0.2	-4.1	2.1	4.3	
61.93	0.6	-4.8	2.4	5.4	
62.93	1.3	-5.6	3.0	6.9	
63.93	2.6	-6.9	4.0	9.5	
64.93	5.0	-9.6	6.0	14.6	

(1)	(2)	(3)	(4)	(5)	(6)
Run 8 Eccentricity =				= 0.0260"	
29.12	−0.7	−1.3	0.1	0.6	.0206
39.32	−0.8	−1.9	0.3	1.1	.0280
43.67	−0.6	−2.9	0.6	2.3	.0463
54.67	−0.1	−3.5	1.2	3.4	.0621
56.67	+0.1	−4.0	1.5	4.1	.0723
58.67	0.7	−4.7	2.0	5.4	.0920
59.93	1.2	−5.2	2.4	6.4	.1069
60.93	1.8	−5.8	3.0	7.6	.1248
61.93	2.4	−6.6	3.5	9.0	.1454
62.93	3.7	−7.9	4.5	11.6	.1845
63.93	5.4	−9.9	6.0	15.3	.2395
64.43	6.9	−11.4	7.0	18.3	.2840

(1)	(2)	(3)	(4)	(5)	(6)
Run 9 Eccentricity =				= 0.0312"	
29.12	−0−	−1.9	0.2	1.9	
39.32	+0.1	−2.8	0.5	2.9	
44.82	0.3	−3.2	0.7	3.5	
49.67	0.8	−4.1	1.3	4.9	
52.67	1.2	−4.8	1.7	6.0	
54.67	1.8	−5.2	2.1	7.0	
56.67	2.3	−6.0	2.5	8.3	
58.67	3.2	−7.1	3.8	10.3	
59.93	4.0	−8.0	4.0	12.0	
60.93	4.9	−9.0	4.6	13.9	
61.93	6.1	−10.8	5.7	16.4	

(1)	(2)	(3)	(4)	(5)	(6)
Run 10	Eccentricity =			= 0.0364"	
29.12	0.5	-2.5	0.2	2.3	.0061
39.82	1.1	-3.6	0.7	4.7	.1196
44.82	1.3	-4.3	1.1	5.6	.1265
49.67	2.2	-5.5	1.8	7.7	.1550
52.67	2.9	-6.3	2.4	9.2	.1746
54.67	3.5	-7.1	3.0	10.6	.1957
56.67	4.4	-8.2	3.3	12.6	.2220
58.67	5.8	-9.8	4.6	15.6	.2660
59.93	7.1	-11.1	5.6	18.2	.3035

(1)	(2)	(3)	(4)	(5)	(6)
Run 11	Eccentricity =			= 0.0416"	
29.12	0.7	-2.5	0.3	3.2	
39.32	1.2	-3.8	0.8	5.0	
44.32	1.7	-4.6	1.2	6.3	
49.67	2.4	-5.8	2.0	8.2	
52.67	3.2	-6.7	2.5	9.9	
54.67	4.0	-7.5	3.0	11.5	
56.67	4.8	-8.7	3.7	13.5	
58.67	6.2	-10.2	5.0	16.4	

(1)	(2)	(3)	(4)	(5)	(6)
Run 12	Eccentricity =			= 0.0520"	
29.12	0.9	-2.8	0.8	3.7	.1271
39.32	1.4	-4.1	1.0	5.5	.1400
44.32	2.2	-5.0	1.5	7.2	.1625
49.67	3.0	-6.2	2.0	9.2	.1850
52.67	3.8	-7.2	2.7	11.0	.2085
54.67	4.6	-8.1	3.5	12.7	.2320
56.67	5.7	-9.6	4.2	15.3	.2697
58.67	7.3	-11.2	5.5	18.5	.3147
59.93	8.8	-12.9	6.5	21.7	.3620

Model D

Steel 3.5" root depth 0.5" tip depth 0.120" thickness

(1)	(2)	(3)	(4)	(5)	(6)
Critical Run Eccentricity = = 0"					
8.5					
67.3					
92.41					
116.64					
140.95					
164.87					
175.24					
185.49					
190.49					

(1)	(2)	(3)	(4)	(5)	(6)
Run 1 Eccentricity = = 0.0013					
67.3	-0.9	-0.9	-0-	-0-	
116.64	-1.5	-1.5	+0.1	-0-	
164.87	-2.0	-2.2	0.1	0.2	.0012
175.24	-2.0	-2.3	0.1	0.3	.0017
185.49	-1.7	-3.1	0.5	1.4	.0076
187.49	-0.7	-4.0	1.3	3.3	.0176
188.47	+0.7	-5.4	2.5	6.1	.0324

(1)	(2)	(3)	(4)	(5)	(6)
Run 2	Eccentricity =			= 0.0026"	
67.3	-0.9	-0.9	-0-	-0-	
116.64	-1.5	-1.5	-0-	-0-	
164.87	-1.9	-2.2	+0.2	+0.3	.0018
175.87	-1.8	-2.7	0.3	0.9	.0051
178.87	-1.8	-2.9	0.5	1.1	.0061
180.87	-1.7	-3.0	0.6	1.3	.0072
182.87	-1.5	-3.2	0.8	1.7	.0093
184.87	-1.1	-3.5	1.1	2.4	.0130
185.87	-0.9	-3.9	1.2	3.0	.0162
186.37	-0.7	-4.1	1.5	3.4	.0182
186.87	-0.5	-4.3	1.7	4.0	.0214
187.37	-0-	-4.9	2.0	4.9	.0261
187.87	+0.5	-5.5	2.4	5.8	.0309
188.37	1.2	-6.1	3.1	7.3	.0388
188.87	2.6	-7.2	4.0	9.8	.0519

(1)	(2)	(3)	(4)	(5)	(6)
Run 3	Eccentricity =			= 0.0052"	
67.3	-0.9	-0.9	-0-	-0-	
116.64	-1.3	-1.6	-0-	+0.3	.0026
164.87	-1.8	-2.4	+0.3	0.6	.0036
175.24	-1.4	-3.0	0.5	1.6	.0091
178.24	-1.2	-3.1	0.6	1.9	.0107
180.24	-1.1	-3.4	1.0	2.3	.0128
182.24	-0.9	-3.9	1.1	3.0	.0164

(1)	(2)	(3)	(4)	(5)	(6)
Run 3 (cont'd) Eccentricity =				= 0.0052"	
184.24	−0.2	−4.3	1.6	4.1	.0222
185.49	+0.3	−5.1	2.2	5.4	.0291
186.99	1.2	−6.0	3.0	7.2	.0386
187.49	3.4	−8.1	4.5	11.5	.0614

(1)	(2)	(3)	(4)	(5)	(6)
Run 4 Eccentricity =				= 0.0078"	
67.3	−0.9	−1.0	−0−	0.1	.0015
116.64	−1.3	−1.7	+0.2	0.4	.0034
164.87	−1.4	−2.8	0.3	1.4	.0085
169.87	−1.3	−3.0	0.4	1.7	.0100
175.24	−1.1	−3.2	0.6	2.1	.0120
178.24	−0.9	−3.7	1.1	2.8	.0157
180.24	−0.6	−4.0	1.4	3.4	.0189
182.24	−0.2	−4.4	1.6	4.2	.0230
183.24	+0.2	−4.9	2.0	5.1	.0278
184.24	0.7	−5.3	2.4	6.0	.0326
185.49	1.7	−6.3	3.1	8.0	.0431
186.49	3.1	−7.8	4.0	10.9	.0584

(1)	(2)	(3)	(4)	(5)	(6)
Run 5	Eccentricity =			= 0.0104"	
67.3	-0.9	-1.0	-0-	0.1	.0015
116.64	-1.3	-1.7	+0.1	0.4	.0034
140.95	-1.5	-2.1	0.1	0.6	.0043
164.87	-1.7	-2.7	0.2	1.0	.0061
169.87	-1.4	-2.8	0.3	1.4	.0082
175.24	-1.3	-3.1	0.6	1.8	.0103
178.24	-1.1	-3.4	1.0	2.3	.0129
180.24	-0.9	-3.8	1.2	2.9	.0161
182.24	-0.5	-4.1	1.4	3.6	.0197
184.24	+0.1	-4.9	2.0	5.0	.0271
185.24	0.8	-5.5	2.5	6.3	.0340

(1)	(2)	(3)	(4)	(5)	(6)
Run 6.	Eccentricity =			= 0.0156"	
67.3	-0.8	-1.1	-0-	0.3	.0045
116.64	-1.1	-1.9	-0-	0.8	.0069
140.95	-1.2	-2.5	+0.3	1.3	.0092
164.87	-0.9	-3.2	0.7	2.3	.0140
169.87	-0.8	-3.7	1.0	2.9	.0171
175.24	-0.2	-4.1	1.4	3.9	.0222
178.24	+0.2	-4.8	1.7	5.0	.0280
180.24	0.7	-5.2	2.1	5.9	.0327
181.24	1.0	-5.7	2.5	6.7	.0370
182.24	1.6	-6.0	2.7	7.6	.0417
183.24	2.2	-6.8	3.1	9.0	.0491
184.24	2.9	-7.6	3.5	10.5	.0570
185.24	4.1	-8.9	4.7	13.0	.0701

(1)	(2)	(3)	(4)	(5)	(6)
	Run 7	Eccentricity =		= 0.0203"	
67.3	-0.4	-1.3	0.1	0.9	.0134
92.41	-0.3	-2.0	0.3	1.7	.0184
116.64	-0.2	-2.7	0.5	2.5	.0214
132.01	-0.1	-3.2	0.6	3.1	.0235
140.95	+0.1	-3.7	1.0	3.8	.0270
151.32	0.4	-4.2	1.2	4.6	.0304
156.32	0.8	-4.7	1.5	5.5	.0352
161.57	1.2	-5.1	1.8	6.3	.0390
166.57	1.8	-5.9	2.2	7.7	.0462
169.57	2.2	-6.4	2.6	8.6	.0507
171.86	2.8	-7.0	3.2	9.8	.0570
173.86	3.3	-7.8	3.5	11.1	.0639
174.86	3.8	-8.0	3.7	11.8	.0675
175.86	4.2	-8.6	4.1	12.8	.0728
176.86	4.7	-9.0	4.6	13.7	.0775
177.86	5.2	-9.7	5.0	14.9	.0838

(1)	(2)	(3)	(4)	(5)	(6)
Run 8		Eccentricity =		= 0.0260″	
67.30	0.2	-1.9	0.2	2.1	.0312
92.41	0.4	-2.8	0.4	3.2	.0346
116.64	0.9	-3.8	0.8	4.7	.0403
132.01	1.4	-4.7	1.2	6.1	.0461
140.95	1.9	-5.3	1.5	7.2	.0511
151.32	2.7	-6.2	2.1	8.9	.0588
161.57	4.1	-8.1	3.2	12.2	.0755
164.87	4.7	-8.8	3.5	13.5	.0820
167.87	5.5	-9.8	4.2	15.3	.0912
169.87	6.2	-10.3	4.9	16.5	.0972
171.87	7.1	-11.3	5.5	18.4	.1075
174.24	8.9	-13.3	6.8	22.2	.1273

(1)	(2)	(3)	(4)	(5)	(6)
Run 9		Eccentricity =		= 0.0312″	
67.30	0.3	-2.2	0.2	2.5	.0372
92.41	0.8	-3.1	0.4	3.9	.0422
107.78	1.2	-3.9	0.8	5.1	.0473
116.64	1.5	-4.3	1.0	5.8	.0498
132.01	2.1	-5.3	1.3	7.4	.0560
140.95	2.7	-6.1	1.8	8.8	.0625
151.32	3.7	-7.3	2.5	11.0	.0726
156.32	4.3	-8.1	3.1	12.4	.0793
161.57	5.3	-9.3	3.9	14.6	.0904
166.57	6.8	-10.9	5.0	17.7	.1062

(1)	(2)	(3)	(4)	(5)	(6)
Run 10		Eccentricity =		= 0.0364"	
67.30	0.4	-2.2	0.2	2.6	.0386
92.41	0.9	-3.1	0.4	4.0	.0433
107.78	1.2	-3.8	0.6	5.0	.0464
116.64	1.5	-4.3	0.8	5.8	.0493
140.95	2.7	-6.1	1.7	8.8	.0625
151.32	3.7	-7.3	2.4	11.0	.0726

(1)	(2)	(3)	(4)	(5)	(6)
Run 11		Eccentricity =		= .0416"	
67.30	0.6	-2.2	0.2	2.8	.0416
92.41	1.0	-3.2	0.4	4.2	.0455
107.78	1.3	-4.0	0.7	5.3	.0492
116.64	1.8	-4.6	1.0	6.4	.0550
132.01	2.3	-5.4	1.4	7.7	.0582
140.95	2.9	-6.3	1.8	9.2	.0653
151.32	4.0	-7.7	2.6	11.7	.0772
161.57	5.9	-9.8	4.0	15.7	.0972
166.57	7.2	-11.2	5.2	18.4	.1104

(1)	(2)	(3)	(4)	(5)	(6)
Run 12	Eccentricity =		= 0.0520$''$		
67.30	1.1	-2.7	0.2	3.8	.0565
92.41	1.7	-3.9	0.5	5.6	.0607
116.64	2.7	-5.4	1.2	8.1	.0695
140.95	4.5	-7.9	2.3	12.4	.0880
151.32	5.9	-9.7	3.2	15.6	.1030
161.57	8.3	-12.2	5.2	20.5	.1270
171.86	13.6	-18.0	8.8	31.6	.1841

	MODEL C			MODEL D	
Run	Eccentricity	a_i		Eccentricity	a_i
11	0.0416"	27.2		0.0416"	18.2
12	0.0520"	34.6		0.0520"	18.2

MODEL A
P VS. DIFF.

FIG. A

-46-

MODEL A
DIFF/P VS. DIFF

FIG. B

MODEL B
P VS. DIFF

FIG. C

-48-

MODEL B

DIFF./$_P$ VS. DIFF.

FIG. D

P CRITICAL RUN

RUN 1

RUN 2

RUN 4

RUN 6

RUN 8

RUN 10

RUN 12

P (#)

-50-

MODEL C
P VS. DIFF

DIFF

FIG. E

MODEL C

DIFF./$_P$ VS. DIFF.

DIFF./$_P$

RUN 12

RUN 10

RUN 8

RUN 6

RUN 4

DIFF.

FIG. F

-15-

CRITICAL RUN

MODEL D
P VS. DIFF.

P (#)

DIFF.

FIG. G

RUN 1 RUN 2 RUN 3 RUN 4 RUN 6 RUN 7 RUN 8 RUN 11 RUN 12

-52-

MODEL D
DIFF/P VS. DIFF.

FIG. III

MODELS A, B, C, D
α_i vs ECCENTRICITY

MODEL D

MODEL C

MODEL A

MODEL B
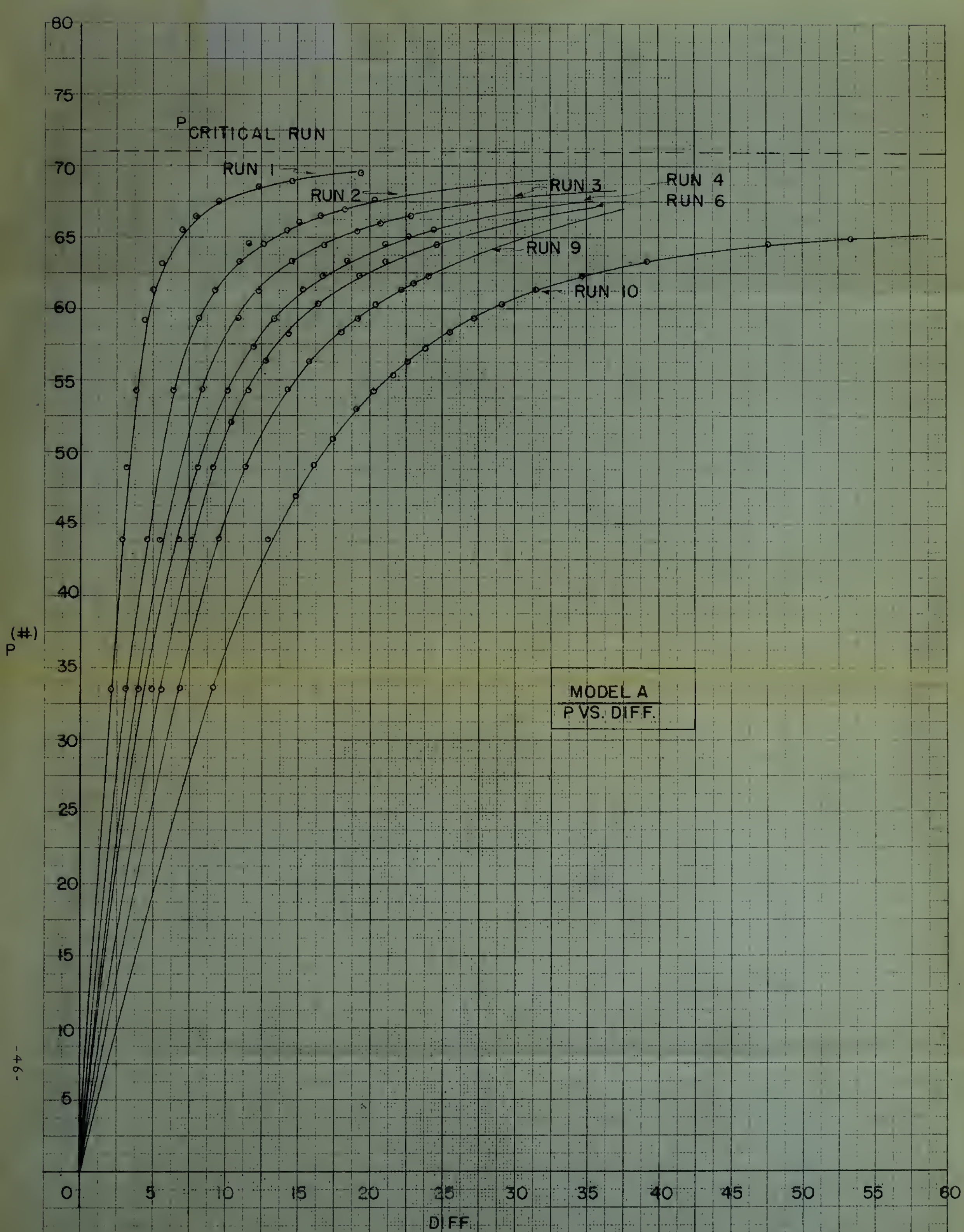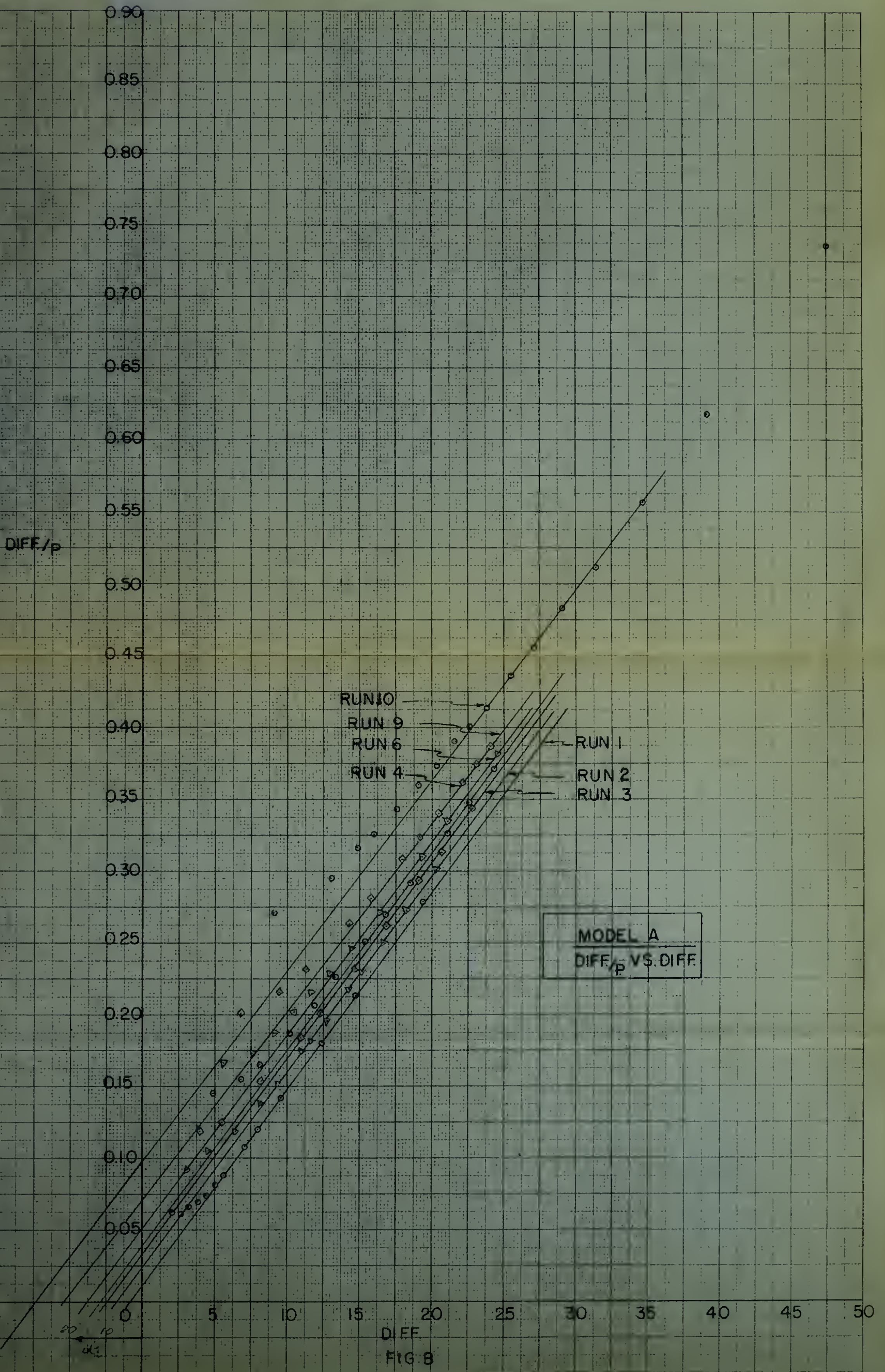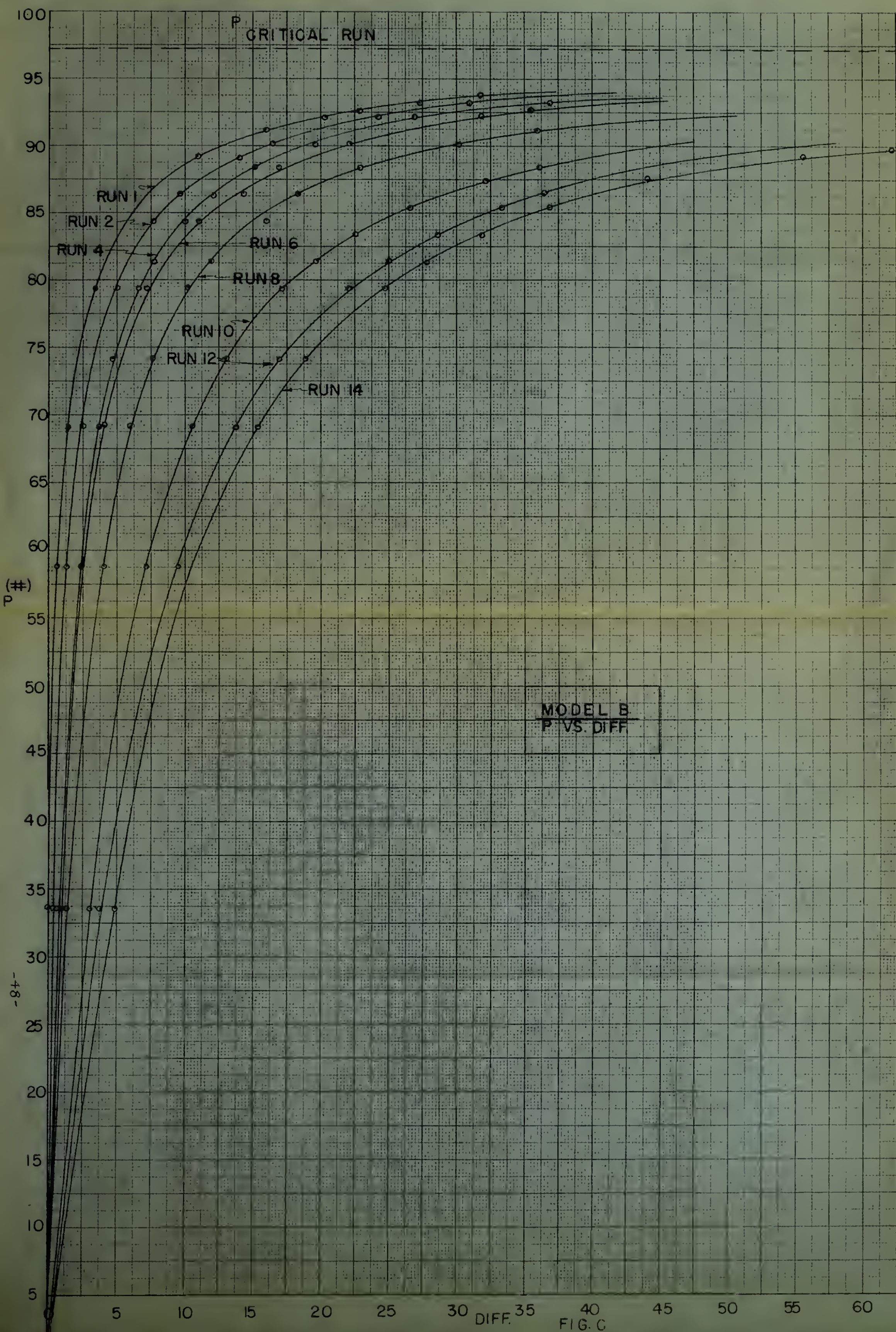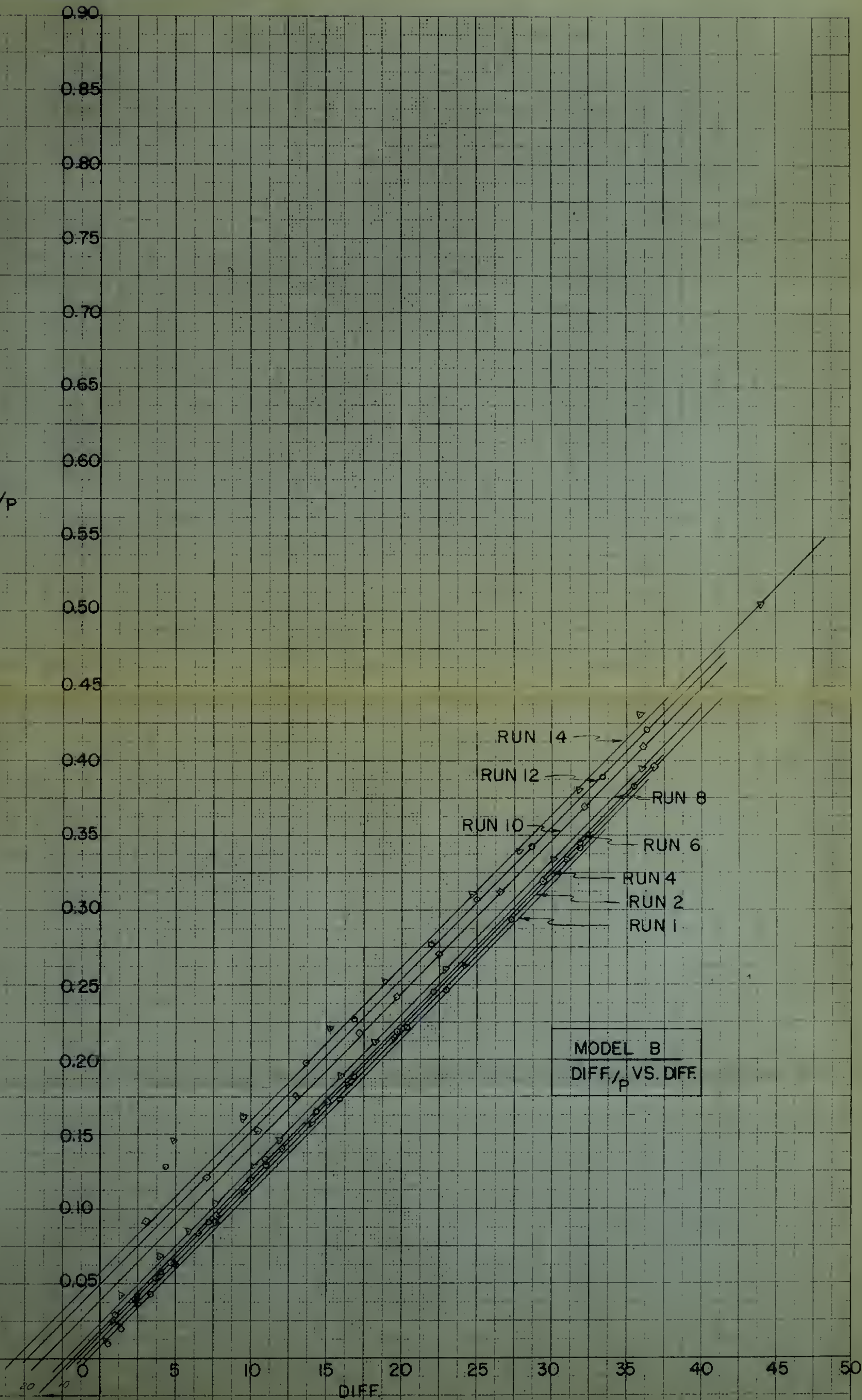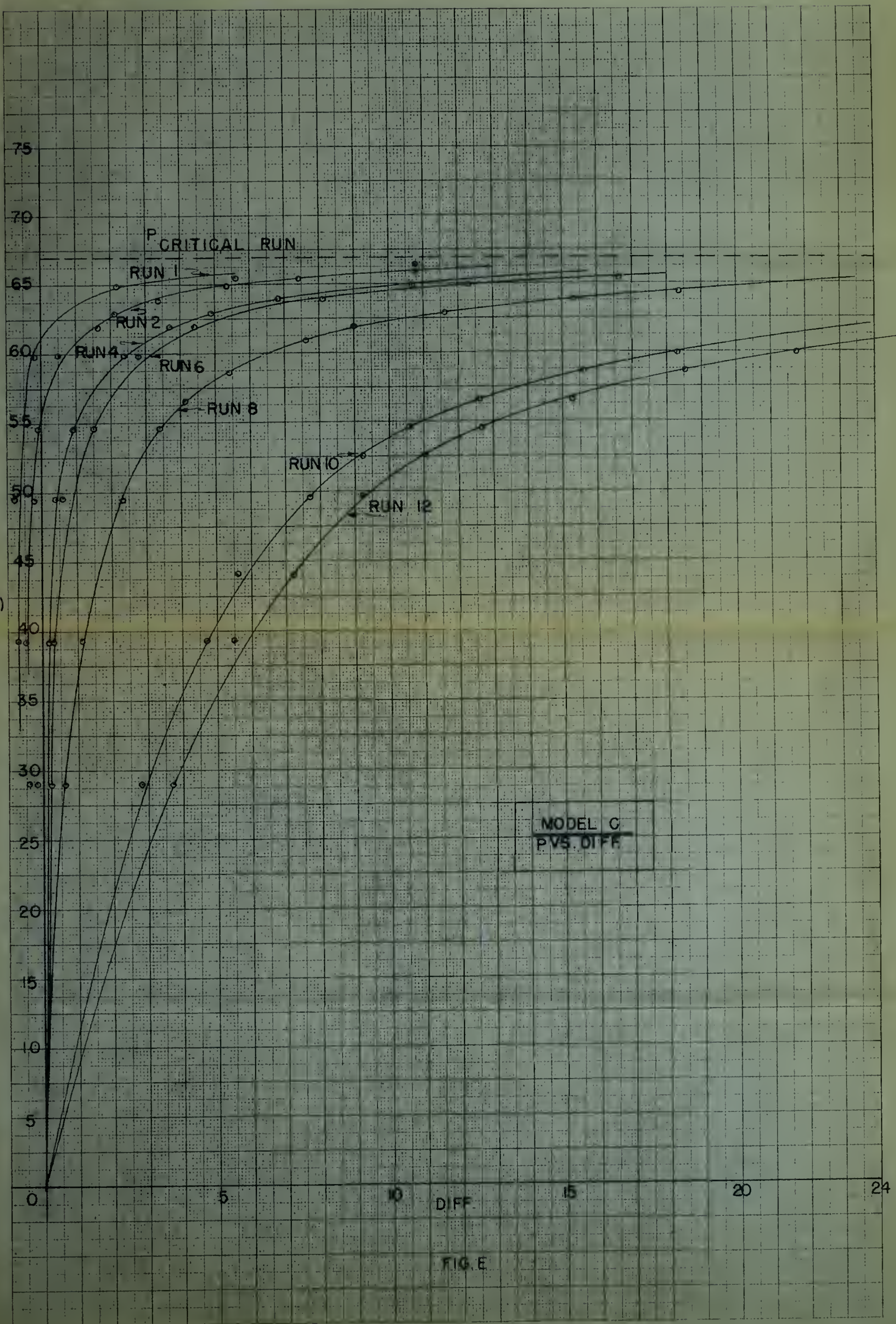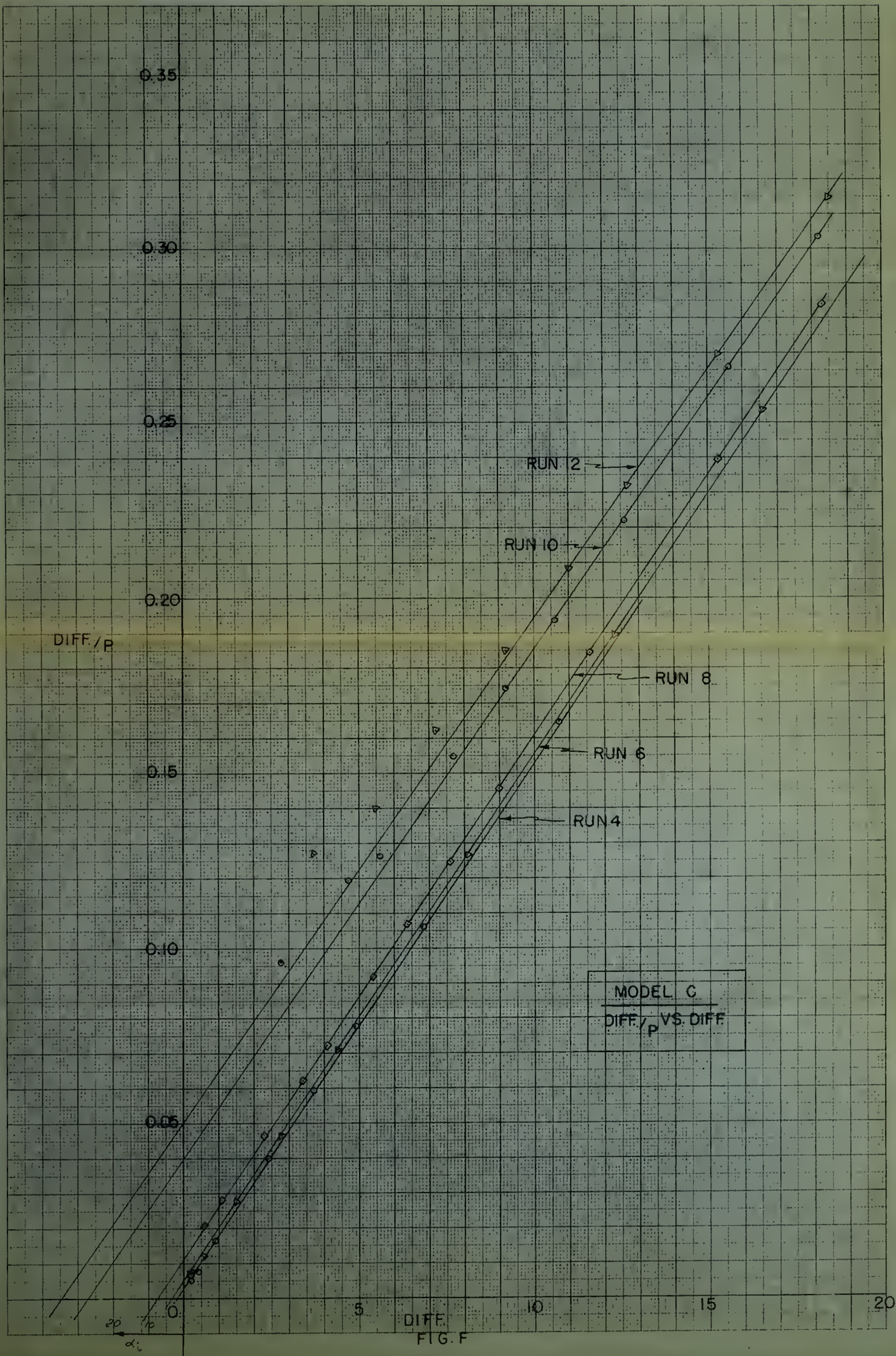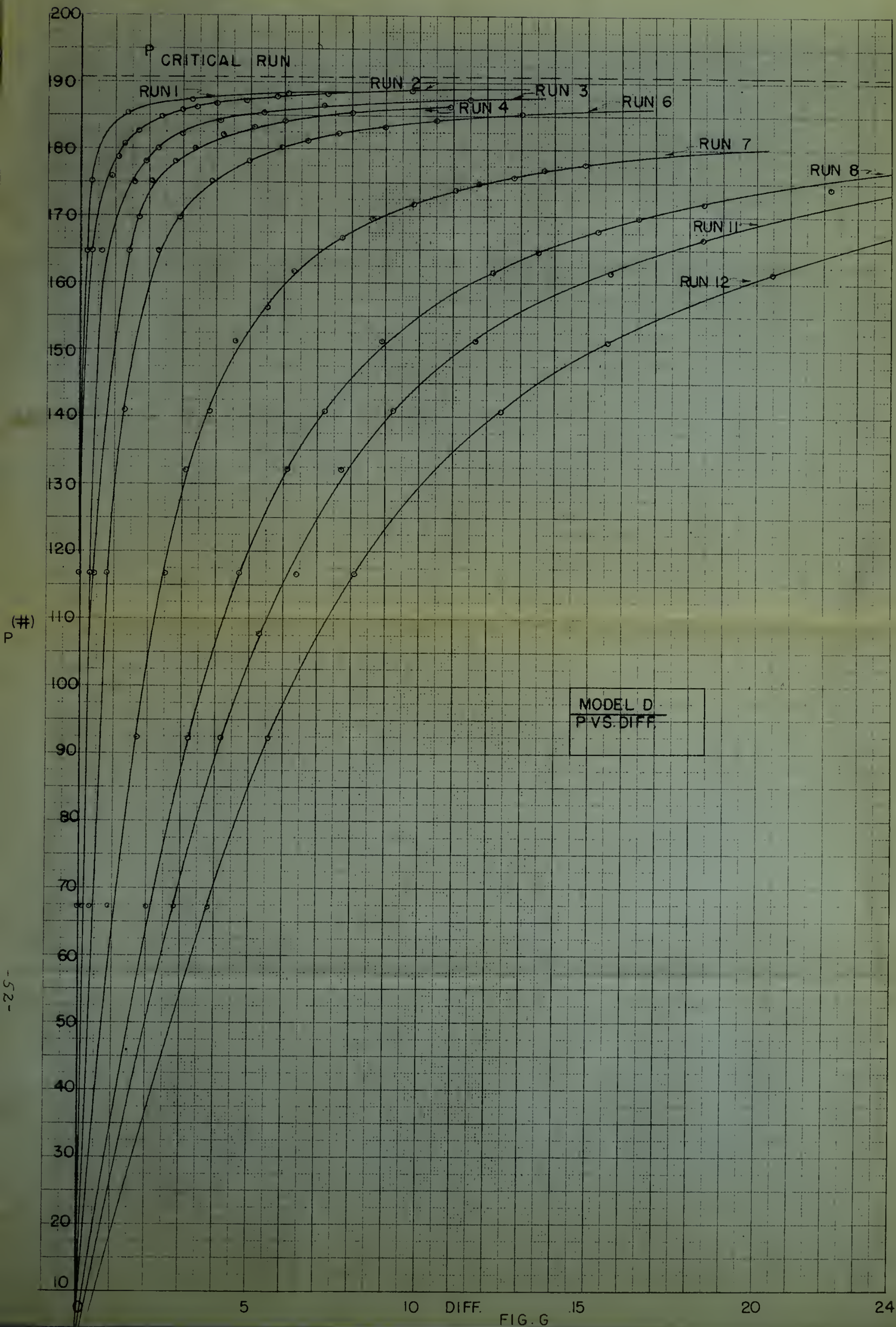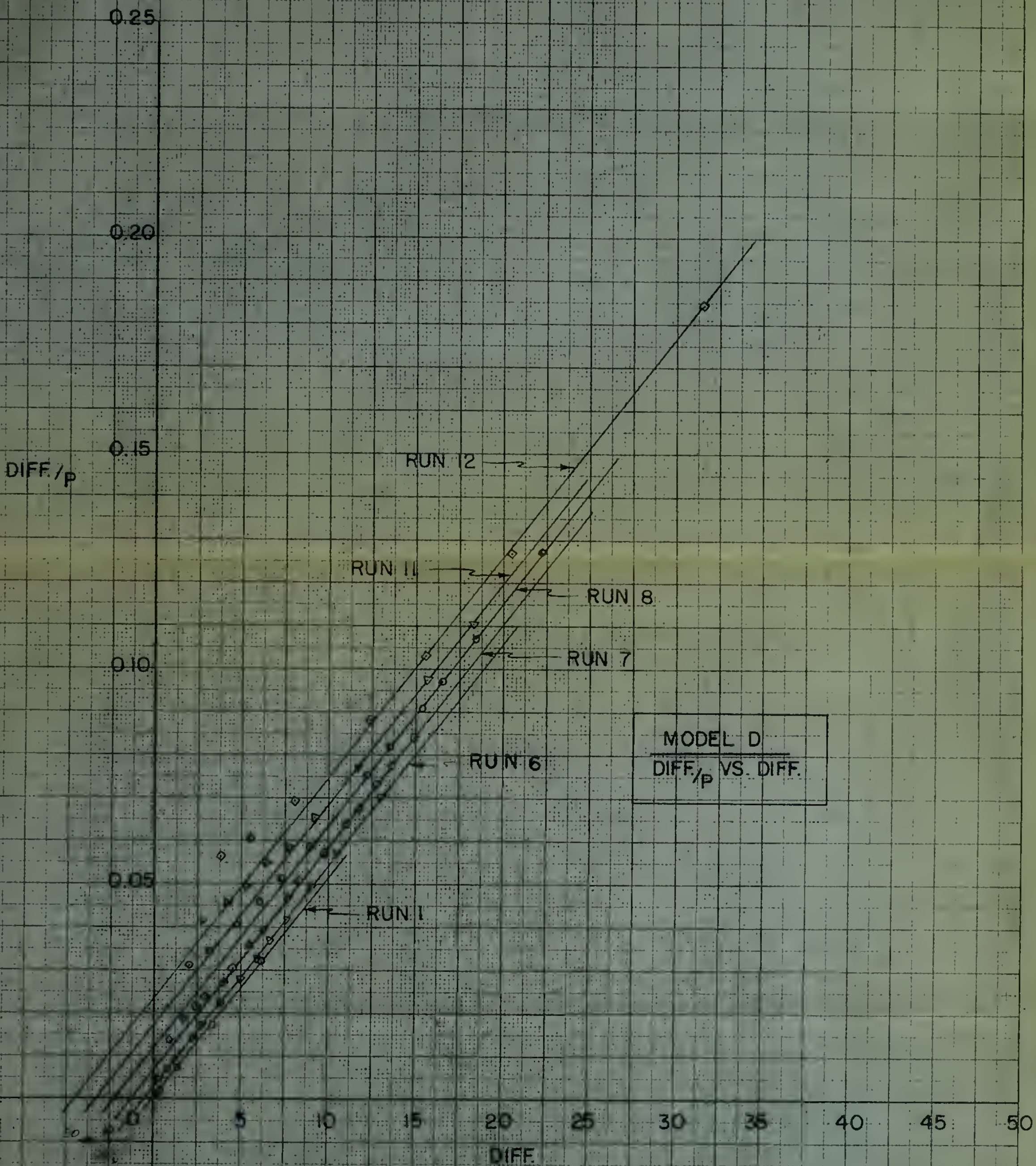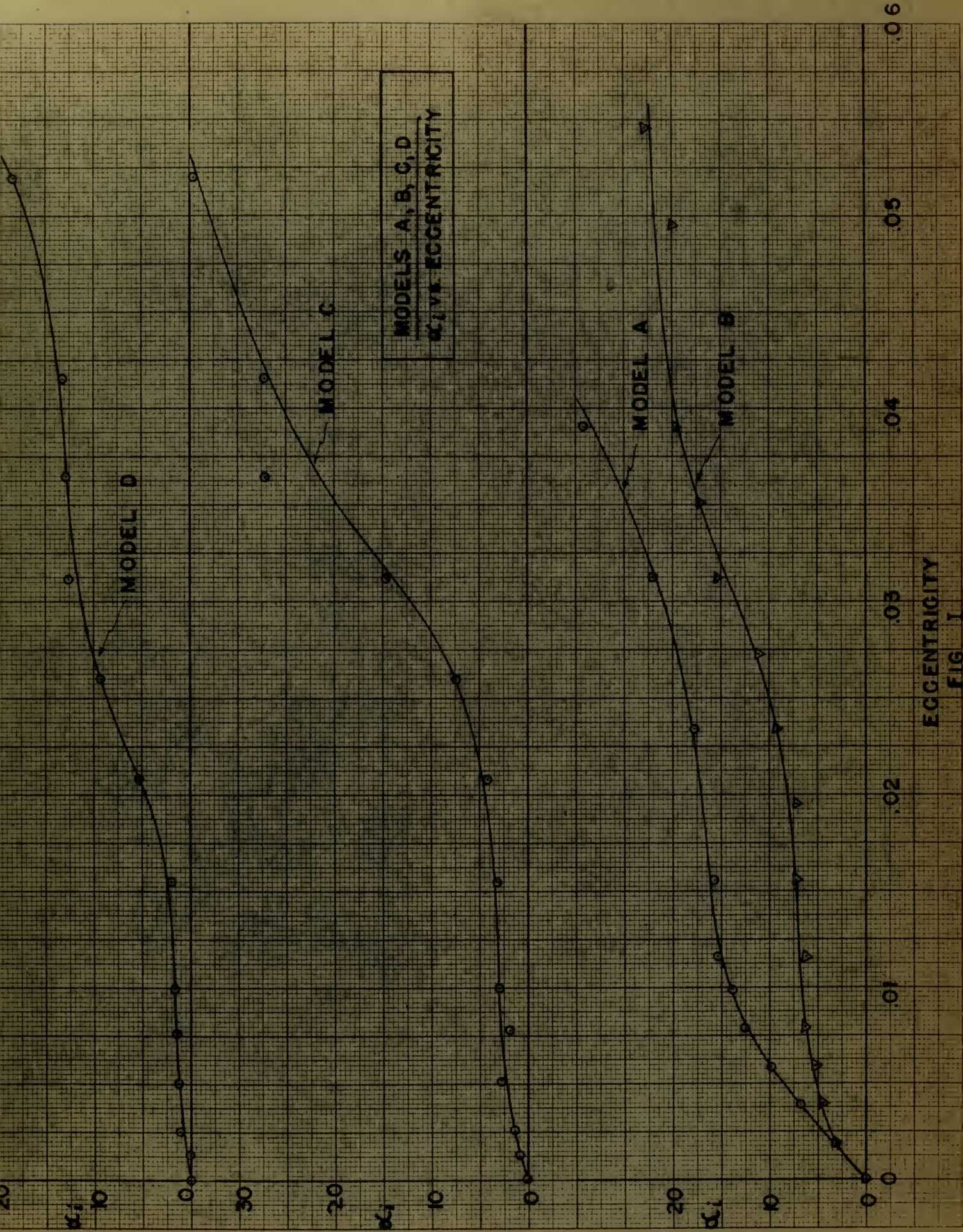
ECCENTRICITY
FIG. I

B. CONCLUSIONS

As indicated in the Introduction, Timoshenko has shown the
theoretical buckling load for the thin cantilever strut tapered to
a point to be:

$$P_{cr} = \frac{m \sqrt{B_1 \, C}}{\ell^2}$$

For struts A and B, where:

$$h = h_o \left(1 - \frac{z}{\ell}\right) \qquad (i.e., \ n = 1)$$

and where a concentrated load is applied at the end, 'm' has a tabulated
value of 2.405 (Reference (1), p. 5), and:

$$\ell = \text{length}$$

$$B_1 = \frac{h \, b^3}{12} \, E$$

$$C = \frac{h \, b^3}{3} \left(1 - 0.630 \, \frac{b}{h}\right) G$$

where: h = depth

             b = thickness

In tabular form:

	ℓ (")	h (")	b (")	E (10^6)	G (10^6)	B_1	C	P_{cr} (lbs)
Model A	18	4.5	0.125	10.5	3.9	7,700	11,200	68.9
Model B	18	6.0	0.125	10.5	3.9	10,280	15,020	92.2

Or, the theoretical buckling loads for models A and B are 68.9 lbs.
and 92.2 lbs., respectively.

Pages 15 to 29 and figures A and C show the data in tabular and
graphical form for models A and B.

Referring to the data, we find the critical loads determined

experimentally for models A and B to be 71 lbs. and 97.2 lbs., respectively. In tabular form:

	Theoretical	Experimental	Exp. % of Theor.
Model A	69.9 lbs.	71.0 lbs.	101.6%
Model B	92.2 lbs.	97.2 lbs.	105.4%

Due to evidence from Southwell's method, shown below, it is believed that these experimental critical loads are very close to the true critical loads.

The difference between the theoretical and experimental values is felt to be due largely to the fact that the portion of the struts at the load end, where the section becomes smallest and where deflections might be expected to be large, had to be reinforced by adding material to resist bending near the end in the yz-plane and to provide a seat for the knife edge. The effect of this reinforcement at the end cannot be accurately taken into account.

Additional factors which might cause minor deviations between the theoretical and experimental values are (1) thickness varying from 0.1245" to 0.1255" throughout the model, (2) use of the material values of E and G, and (3) a possibly slightly longer effective length than 18". (1) is small and enters as the square root of a cube term. (2) enters as a square root.

In view of the manifest impossibility of loading a strut at a point, it is difficult to see how the theory might be checked absolutely. However the small percentage separation of values indicates good correspondence between the experimental and the theoretical values for the type of strut considered.

No formulae for calculating the theoretical critical loads for truncated struts, such as models C and D, have been found. In section II

of this thesis an attempt has been made to derive such a formula, and the experimental critical loads for these models are compared with the critical values calculated.

Figures B, D, F, and H show plots of difference/P vs difference. Southwell has pointed out that in the case of column loads, (1) these lines should be straight and (2) their slopes should equal the critical load, regardless of eccentricity. An extension of this method to the loading under consideration was suggested.

On these figures it will be noted that a set of points from the same run, while having a straight portion, generally curve toward the low end of the set. This curvature has been neglected, and the straight lines have been drawn, with the following explanation.

It will be noted that this deviation from a straight line increases generally with the eccentricity. Now these sets of points will only be in a straight line insofar as they represent points on a hyperbolic curve of P vs difference, (figures A, C, E, and G). Referring to these figures we see that these curves vary from the hyperbolic form in the low range of difference, where they all touch the ordinate at P. For the higher values of P, the curves are very much more truly hyperbolic than for the low values, due to the nature of the curves. Accordingly, only the points at the higher values of difference should be considered in drawing straight lines representing the set of points.

Considering the straight lines approximating the sets of points for various eccentricities, we find the slopes of these lines are approximately parallel for all runs and that they give values of P_{cr} as follows:

$$(\text{Diff.})/(\text{Diff.}/P) \qquad = P_{cr}$$

Model A $(25-5)/(0.3560 - 0.0795) \quad = 72.3$ lbs. (Figure B, Run 1)

Model B $(30-10)/(0.3475 - 0.1420) \quad = 97.2$ lbs. (Figure D, Run 10)

Model C $(15-5)/(0.2550 - 0.0863) \quad = 67.3$ lbs. (Figure F, Run 8)

Model D $(20-10)/(0.6059 - 0.0542) = 193.2$ lbs. (Figure H, Run 6)

Comparing the critical loads determined experimentally with those determined by Southwell's method;

	Experimental	Southwell	South. % of Exp.
Model A	71.0 lbs.	72.3 lbs.	101.8%
Model B	97.2 lbs.	97.2 lbs.	100.0%
Model C	66.9 lbs.	67.3 lbs.	100.7%
Model D	190.7 lbs.	193.2 lbs.	101.4%

we find very close adherence for the models tested. In every case the Southwell lines show a somewhat greater critical. This is considered due to the fact that in loading for critical on the zero line, the true experimental critical loading was not reached.

The conclusion reached, based on the information obtained from these models, is that for these types of strut it is possible to obtain the critical load from a few test points, without first determining the center point of the strut, and without going to loads which might cause the yield strength to be exceeded. In such a determination it will be important, (1) to use a small eccentricity, or (2) to take points from higher loadings only.

The procedure would be to set up the model in a manner similar to that shown herein, place the point of loading fairly close to the model center, apply loads, and measure the deflections (angle of twist)

vs the various loadings. Divide the deflections by the loading and plot vs the deflection. The slope of this line will give the critical load for that strut.

Page 45 gives the tabular form and page 54 gives the graphical form of eccentricity vs a_i, where a_i represents the displacement of the DIFF./P vs DIFF. lines where they cross the DIFF. axis. While a_i is considered as some function of the eccentricity it must be pointed out that considerable error may easily be introduced into the experimental determination of a_i. First, if the eccentricity introduced is not as estimated or calculated, the entire set of values determining the plot of P vs DIFF. will be in error, thus introducing an error in the curves which determine the values of a_i. In the second place, the lines determining a_i (especially for high eccentricities) are approximations to sets of points which do not have a well defined straight portion. An error in the slope of any DIFF./P line will introduce considerable error in the a_i for that eccentricity. a_i should be more representative as a measure of eccentricity for the lower range of eccentricity.

Considering the data shown, we see that the data for models A and B was plotted to the same scale, and hence we should expect some correlation between the curves of a_i vs eccentricity. These curves for models A and B do show a marked degree of similarity. This similarity is emphasized by comparison with the curves for models C and D, whose points are derived from lines drawn to different scales, but which still show the same general trend as models A and B.

From the data available in this experiment it is impossible to tell whether the double curvatures shown in figure I are inherent in the problem, or are due to some consistent error in the experimental setup.

V.   THEORETICAL INVESTIGATION

A.   INTRODUCTION

As a theoretical problem it was proposed to derive a formula that would handle the critical load for lateral buckling of thin struts of constant thickness which are either tapered to a point or truncated. The triangular case has been well presented by Timoshenko in Theory of Elastic Stability. However very little work has been presented for the specific problem of truncated struts. Federhofer (Reference 2) has presented a solution to this problem which is complicated by the fact that it is presented using constants worked out for specific taper ratios. The solution in this paper is considered more flexible in that it may be solved directly by substituting the physical and material values of the model.

In this solution resort was made to Rayleigh's principle which is discussed in the next part, B.

Part C presents the derivation of the formula.

Conclusions are presented in part D.

B.   DISCUSSION OF RAYLEIGH'S PRINCIPLE (REFERENCE 4)

The general idea of Rayleigh's principle is that the potential energy must be equal to the external work done. In relating this to the test for stability we have a structure in equilibrium under load. This will only go out of equilibrium if the setup is acted upon by some disturbing force, called F. The deformation produced will be caused by two energies: W, the work done by the original load and V, the strain potential energy acquired in the deformation. Let E be the work done by the disturbing force and T be the kinetic energy acquired by the setup. By the principle of the conservation of energy we can write:

Reference 4: G.R.J.Temple and W.G.Bickley, "Rayleigh's Principle and Its Applications to Engineering", Oxford University Press, London, 1933.

$$W + E = V + T$$

T will have to be greater than or equal to O. Now if $V > W$, the energy difference, $V - W$, will be supplied by the disturbing forces. Deformation occurs only when these forces are of sufficient magnitude. But if $V \leq W$, the work done by the disturbing forces, no matter how small will all be converted into kinetic energy. Therefore, the criterion for stability is that $V > W$ for all deformations.

The general equilibrium condition for a cantilever beam, loaded as shown below, is

$$A_x \frac{d^2\phi}{dx^2} + \left(\frac{dA_x}{dx} \right) \frac{d\phi}{dx} + \frac{G^2}{C_x} \phi = 0$$
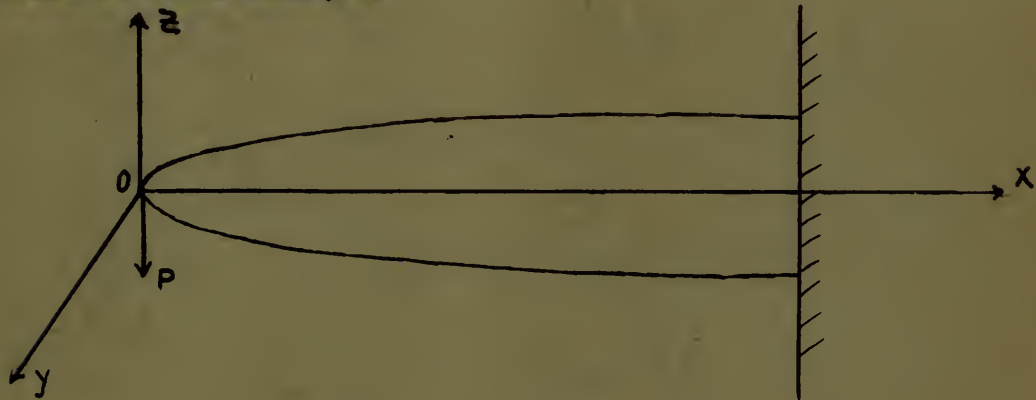
where:

ϕ = the angle of twist

C = flexural rigidity about z-axis

B = flexural rigidity about y-axis

A = torsional rigidity

G = sagging couple

The critical condition for stability is given by:

$$\int_0^\ell A_x \left(\frac{\delta \phi}{\delta x}\right)^2 dx = \int_0^\ell \frac{G^2 \phi^2}{C_x} dx$$

C. SOLUTION FOR CRITICAL LOAD OF TRUNCATED BEAM OF CONSTANT

THICKNESS AND LINEAR TAPER LOADED AS SHOWN
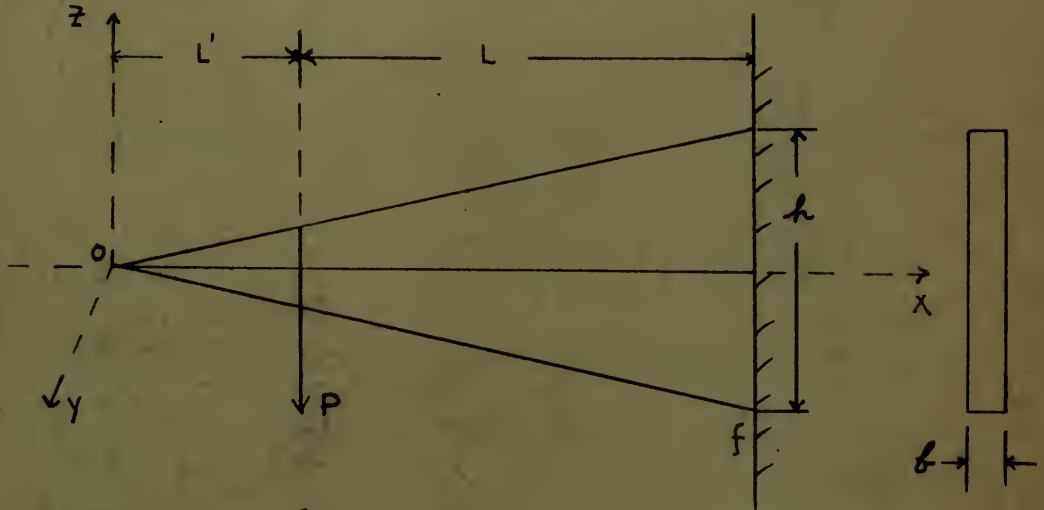
Assumptions:

    1. Within elastic regime.

    2. Torsional rigidity varies linearly.

The flexural rigidity about the z-axis:

$$C = \frac{b\, h\, E}{12} \qquad L' < x < (L' + L).$$

Let:

$$C_f = C \text{ at fixed end.}$$

At any place on the beam:

$$C_x = C_f \left(\frac{x}{L \times L'}\right)$$

The torsional rigidity (Reference 5):

Reference 5: S. Timoshenko, "Theory of Elasticity", p.249, McGraw-Hill, 1934.

$$A = \frac{b^3 h}{3} \left(1 - 0.630 \frac{b}{h} \sum_{n=1,3,5}^{\infty} \frac{1}{n^5} TANH \frac{n \pi h}{2 b} \right) H$$

Let:

$A_f = A$ at fixed end.

At any place on the beam, assume:

$$A_x = A_f \left(\frac{x}{L+L'} \right)$$

The general differential equation for the equilibrium condition is:

$$A_x \frac{d^2 \phi}{d x^2} + \left(\frac{d A_x}{d x} \right) \frac{d \phi}{d x} + \frac{G^2}{C_x} \phi = 0$$

Where:

$$G = P (x - L')$$

Now:

$$\frac{d A_x}{d x} = \frac{A_f}{L+L'}$$

Substituting:

$$A_f \left(\frac{x}{L+L'} \right) \frac{d^2 \phi}{d x^2} + \frac{A_f}{L+L'} \frac{d \phi}{d x} + \frac{P^2 (x-L')^2 (L+L')}{C_f \, x} \phi = 0$$

$$\frac{d^2 \phi}{d x^2} + \frac{1}{x} \frac{d \phi}{d x} + \frac{P^2 (L+L')^2 (x-L')^2}{A_f \, C_f \, x^2} \phi = 0$$

$$\text{let } \beta^2 = \frac{P^2 (L+L')^2}{A_f \, C_f}$$

$$\frac{d^2 \phi}{d x^2} + \frac{1}{x} \frac{d \phi}{d x} + \frac{(x-L')^2}{x^2} \beta^2 \phi = 0$$

By using the following approximate method of solution we will have a

solution of the form

$$\phi = K \, f(x, \, L, \, L')$$

The boundary conditions are:

for ϕ
$\quad x = L'$, $\quad \phi \neq 0$
$\quad x = L + L'$, $\quad \phi = 0$ ←

for ϕ'
$\quad x = L'$, $\quad \phi' = 0$ ←
$\quad x = L + L'$, $\quad \phi' \neq 0$

for ϕ''
$\quad x = L'$, $\quad \phi'' = 0$ ←
$\quad x = L + L'$, $\quad \phi'' = 0$ ←

for ϕ'''

$$\phi''' + \frac{1}{x} \phi'' - \frac{1}{x^2} \phi' + \frac{(x-L')^2}{x^2} \beta^2 \phi' + \frac{x^2 \, 2(x-L') - (x-L')^2 \, 2x}{x^4} \beta^2 \phi = 0$$

$\quad x = L'$, $\quad \phi''' = 0$ ←
$\quad x = L + L'$, $\quad \phi''' \neq 0$

for ϕ^{IV}

$$\phi^{IV} + \frac{1}{x} \phi''' - \frac{2}{x^2} \phi'' + \frac{2}{x^3} \phi' + \frac{(x-L')^2}{x^2} \beta^2 \phi'' + 2 \frac{x^2 \, 2(x-L') - (x-L')^2 \, 2x}{x^4} \beta^2 \phi'$$
$$+ \frac{2x^4 \{3x^2 - 2xL' - 3x^2 + 4L'x - L'^2\} - 8x^3 \{x^2(x-L') - (x-L')^2 x\}}{x^9} \beta^2 \phi = 0$$

$\quad x = L'$, $\quad \phi^{IV} \neq 0$
$\quad x = L + L'$, $\quad \phi^{IV} \neq 0$

Higher order derivatives give no further boundary conditions.

In the differential equation, let:

$$y = x - L'$$

$$\frac{\partial \phi}{\partial x} = \frac{\partial \phi}{\partial y}$$

$$\frac{\partial^2 \phi}{\partial x^2} = \frac{\partial^2 \phi}{\partial y^2}$$

Substituting:

$$\frac{\partial^2 \phi}{\partial y^2} + \frac{1}{y+L'} \cdot \frac{\partial \phi}{\partial y} + \frac{y^2}{(y+L')^2} \beta^2 \phi = 0$$

where y goes from 0 to L.

We have five boundary conditions and therefore select a series assumed to represent ϕ curve of the form:

$$\phi = \frac{K_1}{L^5} (a_0 L^5 + a_1 L^4 y + a_2 L^3 y^2 + a_3 L^2 y^3 + a_4 L y^4 + a_5 y^5)$$

For boundary condition: $y = L$; $\phi = 0$. $L_5 \neq 0$

$$a_0 + a_1 + a_2 + a_3 + a_4 + a_5 = 0$$

$$\phi' = \frac{K_1}{L^5} (a_1 L^4 + 2a_2 L^3 y + 3a_3 L^2 y^2 + 4a_4 L y^3 + 5a_5 y^4)$$

For boundary condition: $y = 0$; $\phi' = 0$ $a_1 = 0$

$$\phi'' = \frac{K_1}{L^5} (2a_2 L^3 + 6a_3 L^2 y + 12a_4 L y^2 + 20a_5 y^3)$$

For boundary condition: $y = 0$, L; $\phi'' = 0$

$$a_2 = 0$$

$$3a_3 + 6a_4 + 10a_5 = 0$$

-65-

$$\phi''' = \frac{K_1}{L^5} (12a_3 L^2 + 24a_4 \, Iy + 60a_5 y^2)$$

For boundary condition: $y = 0$; $\phi''' = 0$

$$a_3 = 0$$

We have two equations with three unknowns.

Solving in terms of a's

$$a_o + a_4 + a_5 = 0$$

$$5a_4 + 5a_5 = 0$$

$$a_4 = -\frac{5}{5} a_5 \qquad\qquad a_1 = 0$$

$$a_o = +\frac{5}{3} a_5 - \frac{3}{3} a_5 \qquad\qquad a_2 = 0$$

$$a_o = \frac{2}{3} a_5 \qquad\qquad a_3 = 0$$

Substituting in ϕ we have:

$$\phi = K_1 \left(\frac{2}{3} a_5 - \frac{5}{3} a_5 \frac{y^4}{L^4} + a_5 \frac{y^5}{L^5} \right)$$

or:

$$\phi = K \left(2 - 5 \frac{y^4}{L^4} + 3 \frac{y^5}{L^5} \right)$$

or substituting for $y = x - L'$:

$$\phi = K \left\{ 2 - 5 \frac{(x - L')^4}{L^4} + 3 \frac{(x - L')^5}{L^5} \right\}$$

$$\phi' = K \left\{ -20 \frac{(x - L')^3}{L^4} + 15 \frac{(x - L')^4}{L^5} \right\}$$

$$\phi'' = K \left\{ -60 \frac{(x - L')^2}{L^4} + 60 \frac{(x - L')^3}{L^5} \right\}$$

Substituting ϕ and ϕ' in critical condition:

$$\int_{L'}^{L+L'} A_x \left(\frac{d\phi}{dx}\right)^2 dx = \int_{L'}^{L+L'} \frac{G^2 \phi^2}{C_x} dx$$

$$G = P(z - L')$$

$$\left(\frac{A_f}{L+L'}\right)\int_{L'}^{L+L'} x K^2 \left\{-20 \frac{(x-L')^3}{L^4} + 15 \frac{(x-L')^4}{L^5}\right\}^2 dx = \frac{L+L'}{C_f} P^2 \int_{L'}^{L+L'} \frac{(x-L')^2 K^2}{x} \left\{2 - 5 \frac{(x-L')^4}{L^4} + 3 \frac{(x-L')^5}{L^5}\right\}^2 dx$$

Let:

$$R = \frac{A_f C_f}{P^2 (L+L')^2} \qquad\qquad K^2 \neq 0$$

Then:

$$R \int_{L'}^{L+L'} x \left\{-20 \frac{(x-L')^3}{L^4} + 15 \frac{(x-L')^4}{L^5}\right\}^2 dx = \int_{L'}^{L+L'} \frac{(x-L')^2}{x} \left\{2 - 5 \frac{(x-L')^4}{L^4} + 3 \frac{(x-L')^5}{L^5}\right\}^2 dx$$

Simplifying:

$$R \int_{L'}^{L+L'} 25 \left\{16 \frac{x(x-L')^6}{L^8} - 24 \frac{x(x-L')^7}{L^9} + 9 \frac{x(x-L')^8}{L^{10}}\right\} dx$$

$$= \int_{L'}^{L+L'} \left\{\frac{4}{x}(x-L')^2 - \frac{20}{xL^4}(x-L')^6 + \frac{12}{xL^5}(x-L')^7 + \frac{25}{xL^8}(x-L')^{10} - \frac{30}{xL^9}(x-L')^{11} + \frac{9}{xL^{10}}(x-L')^{12}\right\} dx$$

Integrating and simplifying:

$$25 \frac{A_f C_f}{P^2(L+L')^2 L^2}\left(\frac{7}{30} + \frac{2}{7}\gamma\right) = \frac{835}{924} - \frac{257}{99}\gamma - \frac{229}{120}\gamma^2 + \frac{239}{84}\gamma^3 - \frac{839}{168}\gamma^4 + \frac{89}{7}\gamma^5$$

$$+ \frac{55}{4}\gamma^6 - \frac{79}{30}\gamma^7 + \frac{19}{4}\gamma^8 - 13\gamma^9 - \frac{51}{2}\gamma^{10} - 9\gamma^{12}$$

$$+ (4\gamma^2 - 20\gamma^6 - 12\gamma^7 + 25\gamma^{10} + 30\gamma^{11} + 9\gamma^{12}) \ln u$$

where:

$$\gamma = \frac{L'}{L} \qquad u = \frac{L + L'}{L'}$$

$$C_f = \frac{b\,h^3}{12}\,E$$

$$A_f = \frac{b\,h^3}{3}\left\{ 1 - 0.630\,\frac{b}{h}\sum_{n=1,3,5\ldots}^{\infty}\frac{1}{n^5}\tanh\frac{n\pi h}{2b}\right\}\,H$$

For triangular struts, $L' = 0$, $\gamma = 0$,

where: $b = \frac{1"}{8}$, $h = 4.5"$, $L = 18"$, $E = 10.5\,(10^6)$, $H = 3.9\,(10^6)$

$$P_{cr} = 72.7 \text{ lbs.}$$

and where: $h = 6.0"$, other values remaining the same:

$$P_{cr} = 97.5 \text{ lbs.}$$

For truncated struts, where: $b_f = b_p = \frac{1"}{8}$ $h_f = 3.5"$ $h_p = 0.5"$

$$L' = 3" \qquad L = 18" \qquad E = 10.5\,(10^6) \qquad H = 3.9\,(10^6)$$

$$P_{cr} = 62.8 \text{ lbs.}$$

and where: $E = 50\,(10^6)$, $H = 11.5\,(10^6)$, other values remaining the same:

$$P_{cr} = 179.3 \text{ lbs.}$$

D. CONCLUSIONS

The theoretical values obtained by use of the formula above may be compared with the experimental values for the various struts tested. In tabular form:

	Experimental	Theoretical	Theor. % of Exp.
Model A	71.0 lbs.	72.7 lbs.	102.3 %
Model B	97.2 lbs.	97.5 lbs.	100.2 %
Model C	66.9 lbs.	62.8 lbs.	93.9 %
Model D	190.7 lbs.	179.3 lbs.	94.1 %

Due to the fact that the models has to be built up at the end (in the case of the triangular struts to prevent bending and to provide a seat for knife edge, and in the case of the truncated struts to provide a seat for knife edge) the theoretical values should be under the experimental value for all struts.

In all cases we have assumed that the torsional rigidity varies linearly with the length. Actually the torsional rigidity varies as follows:

$$C = \frac{b^3 h}{3} \left(1 - 0.630 \frac{b}{h} \sum_{n=1,3,5\cdots}^{\infty} \frac{1}{n^5} \tanh \frac{n\pi h}{2b}\right) H.$$

Examination of the formula shows that for very small values of h, such as occur at the tip of triangular struts, the torsional rigidity becomes smaller than would be predicated by linear variation of torsional rigidity, thus making our theoretical values for these struts high. This explains the greater value of our theoretical over experimental values for models A and B.

For the truncated struts this effect is not so great, and as one would expect the theoretical values are under the experimental values.

VI. REFERENCES

1. S. Timoshenko, "Theory of Elastic Stability", p. 249, 250,

    McGraw - Hill, 1936.

2. K. Federhofer, "Reports International Congress for Applied

    Mechanics", Stockholm, 1930.

3. R. V. Southwell, "Proceedings Royal Society", London, Series A,

    Vol. 135, p. 60, 1932.

4. G. F. J. Temple and W. G. Bickely, "Rayleigh's Principle and Its

    Applications to Engineering", Oxford

    University Press, London, 1933.

5. S. Timoshenko, "Theory of Elasticity", p. 249, McGraw - Hill, 1934.

6. A. Dinnik, A.S.M.E. Trans., Vol. 51, p. 11.

A. N. Proctor, Engineering, Vol. 144, p.62-62, 116-118, 184-186.

APPENDIX A - Specimen Drawings

All models-
thickness

Model A

2" ←| |←————— 18" —————→|

24ST
Aluminum   ⊄

4.5"

see end
detail below

1"→ |←

Model B

2"→| |←————— 18" —————→|

6"   24ST
Aluminum   ⊄

see end
detail below

1"→ |←

Model C

2"→| |←————— 18" —————→|

.5"   24ST   0.5"
Aluminum   ⊄

see end
detail below

1"→ |←
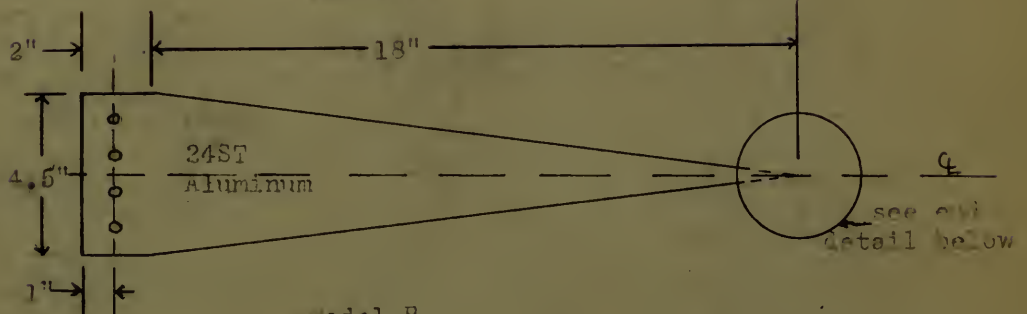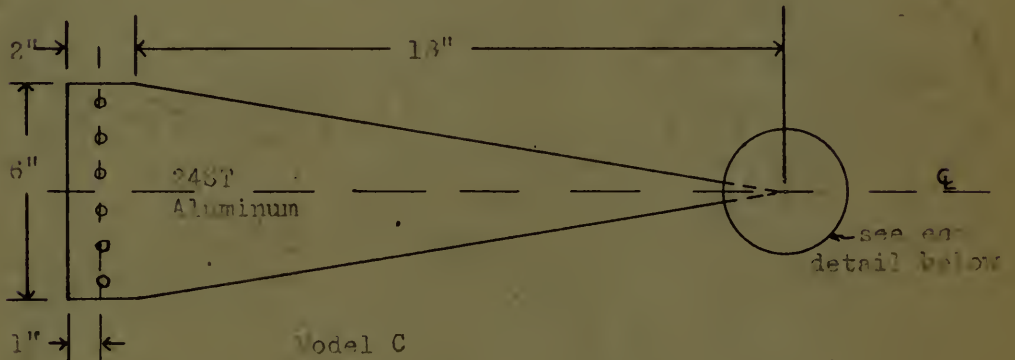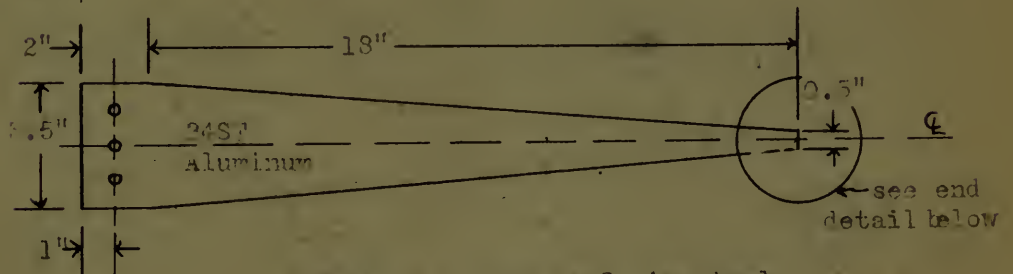
Model D - same as C, in steel

Model End Detail (not to scale).

End of model

Truncated   ½"
                                                  — ⊄ of model
Pointed

5/16"→

Knife edge seat

9/16"
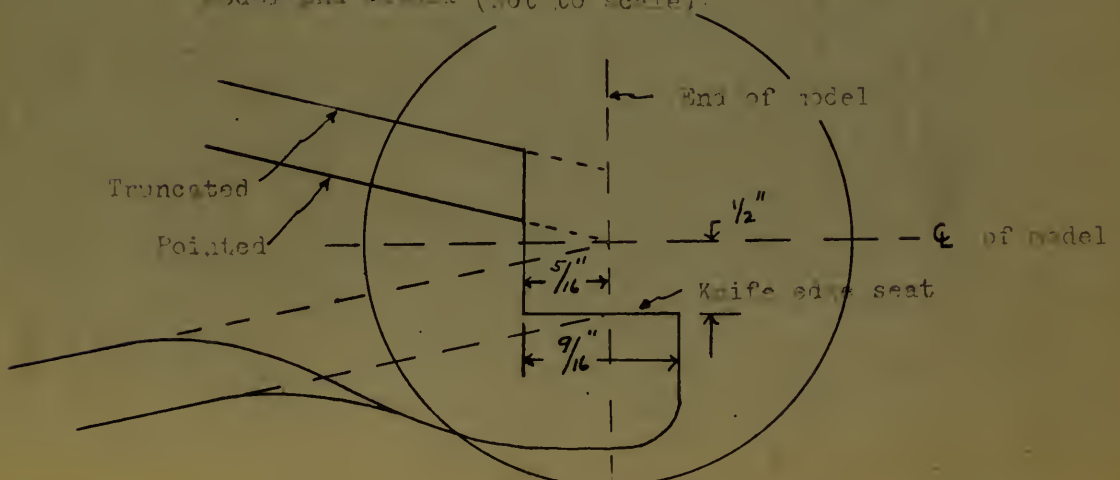
APPENDIX B - Drawings of Physical Setup

Side View

heavy
Steel
Backing

Pointer

Knife
Edge

Top View

Pointer
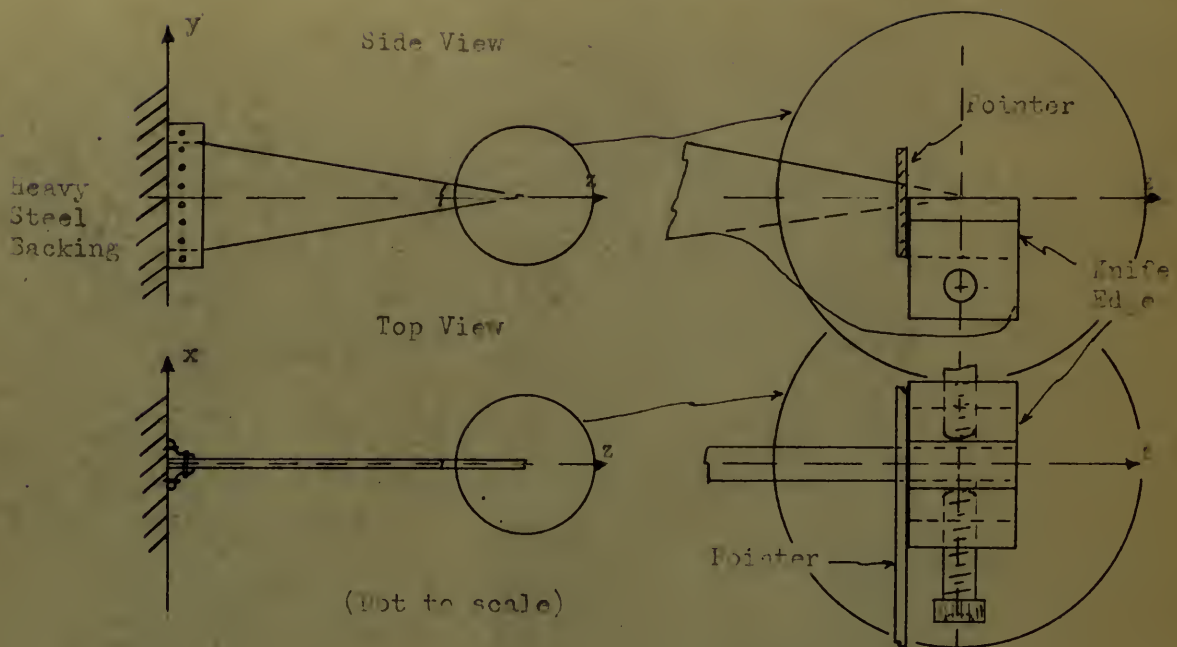
(Not to scale)

Detail of Knife Edge (Full size)

¼"

7/16"

3/4"

½"

¼"

¼"
RADIUS

1¼"

½"

½"

½"

10/32 Nat. fine, with Allen head
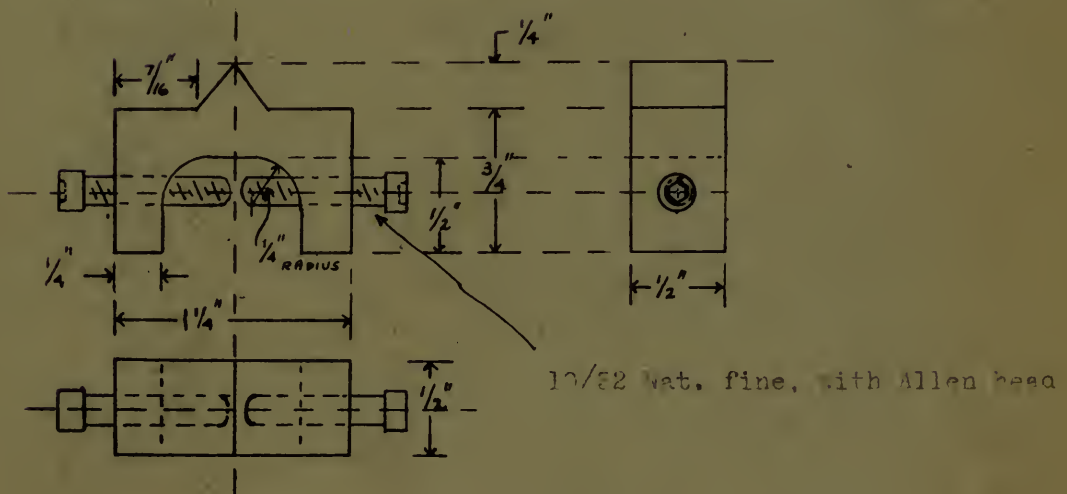
Suggested design for screw end (Not to scale)

Bearing
area
ground
flat

Screw

Cup and ball point

-72-
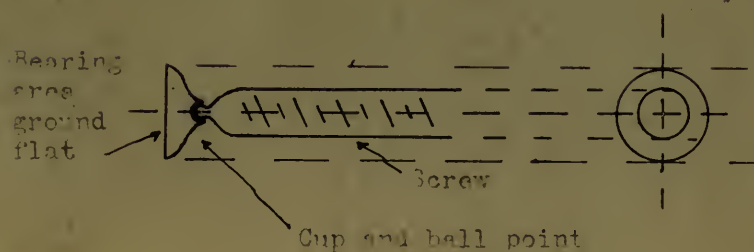
Detail of Pointer - (Not to scale)

Mat'l - Spring brass

¼"

30"

¹⁄₆₄"

Clips sweated on
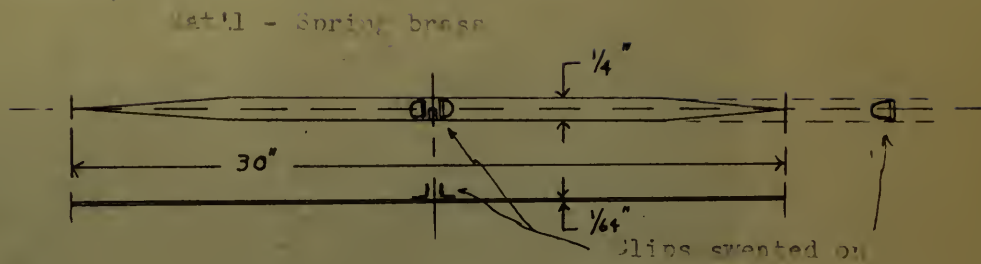
Indicating system - (Not to scale)

+ x

+ y

millimeter graph paper

-y

-x
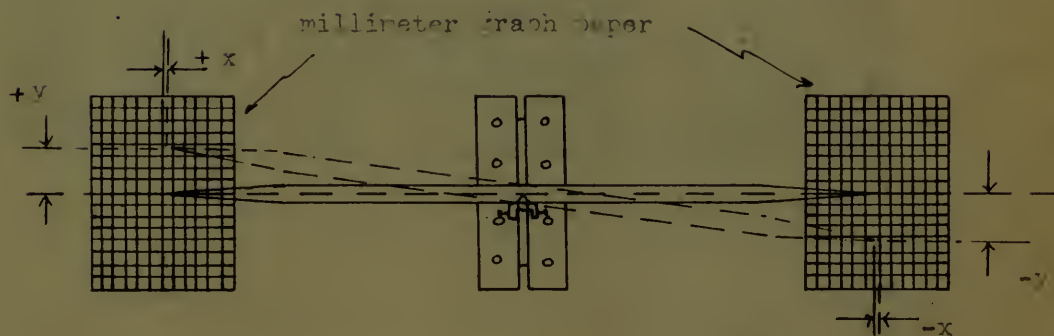
Detail of Loading Rig - (Not to scale)

saddle

knife edge seat

steel straps

piano wire

steel pan
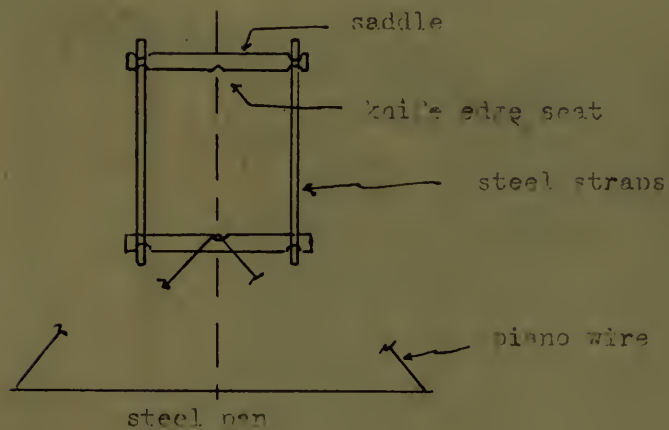
1. Detail of knife edge

2. Detail of fixed end

4. Setup under load

3. General experimental setup

β vs. DIFF.

APPENDIX D

-76-

DATE DUE